國立中山大學
National Sun Yat-sen University

VŠB TECHNICKÁ UNIVERZITA OSTRAVA

2026 International Energy and Environment Conference

A Study on Enhancing the Thermal Management System Control of Fuel Cell Hybrid Electric Vehicles Using the Sparrow Search Algorithm

Department of Mechanical and Electro-Mechanical Engineering
National Sun Yat-sen University, Kaohsiung, 804201, Taiwan

Presenter: Prof. **Jenn-Kun Kuo**

Date: 07-09 September 2026

Hydrogen and Fuel Cell Laboratory
氫能與燃料電池實驗室

Outline

1 Introduction

- Background
- Literature review
- Research Motivation and objectives

2 Research Methodology

- Vehicle Structure
- Subsystem Introduction
- Surrogate Model Development
- SSA and Fuzzy PI Control

3 Model Validation

- Test Cycle Verification
- System Verification

4 Results and Discussion

- Vehicle System Performance
- PI Controller Optimization at Different Speeds
- Fuzzy Gain-Scheduling Control Results
- Comparison of Thermal Management Strategies

5 Conclusion

6 Reference

PEMFC THERMAL MANAGEMENT: RESEARCH EVOLUTION

From component-level control to vehicle-level intelligent optimization

THERMAL MANAGEMENT MODELING & CONTROL

FROM COMPONENT CONTROL TO VEHICLE INTEGRATION

2010 · Hu et al. [6]

Incremental Fuzzy Control

- Coolant flow + bypass valve
- 343 K; max deviation 1.3 K
- Better disturbance rejection than PI

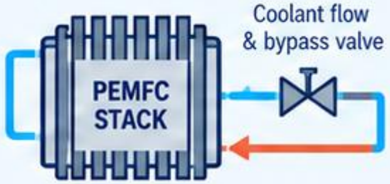

2015 · Han et al. [2]

75-kW Dynamic Cooling Model

- Pump, fan and bypass strategies
- Fan dominates parasitic power
- Temperature + energy co-optimization

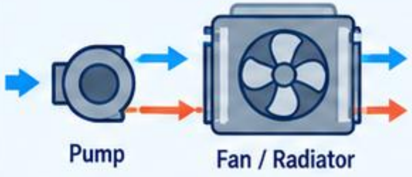

2015 · Cheng et al. [3]

Fuel-Cell Bus Control

- Feedforward + feedback
- Vehicle-test validation
- Coolant maintained near target

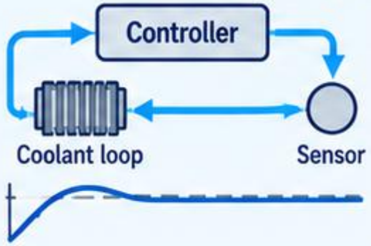

2020 · Xu et al. [1]

Integrated Vehicle Thermal Model

- Stack + intake air + traction motor
- Coupled vehicle-level management

CURRENT RESEARCH FRONTIER

- Vehicle-level multi-source thermal coupling
- Temperature-parasitic energy co-optimization
- Intelligent adaptive control
- Variable-load and real-vehicle validation

INTELLIGENT OPTIMIZATION

FROM ALGORITHM DEVELOPMENT TO CONTROL APPLICATION

2020 · Xue & Shen [4]

Sparrow Search Algorithm (SSA)

- Producer, scrounger and aware roles
- Global exploration + local exploitation

2022 · Xu et al. [5]

SSA-Optimized PID

- Faster temperature tracking
- Better dynamic response
- Stronger disturbance rejection

Vehicle Introduction

Hyundai Elec City Fuel Cell		
Components	**Value**	**Unit**
Length	10995	mm
Width	2490	mm
Height	3400	mm
Gross Vehicle Weight	16,000	kg
Wheel Radius	0.47	m
Drive	Rear-wheel drive	-

This study investigates the thermal management control of a fuel cell electric bus under varying vehicle speeds and thermal loads. Since a fixed-gain PI controller cannot fully accommodate low , medium , and high-speed operating conditions, it may result in insufficient cooling performance or excessive parasitic power consumption from the coolant pump and radiator fan.

Therefore, this study divides the vehicle operating range into several speed regions and applies the Sparrow Search Algorithm to optimize the PI parameters for each region. Fuzzy logic is then introduced to schedule the controller gains smoothly according to vehicle speed. The objective is to maintain stable stack temperature while reducing cooling-system parasitic power consumption and improving the overall energy efficiency of the fuel cell electric bus.

Vehicle Structure

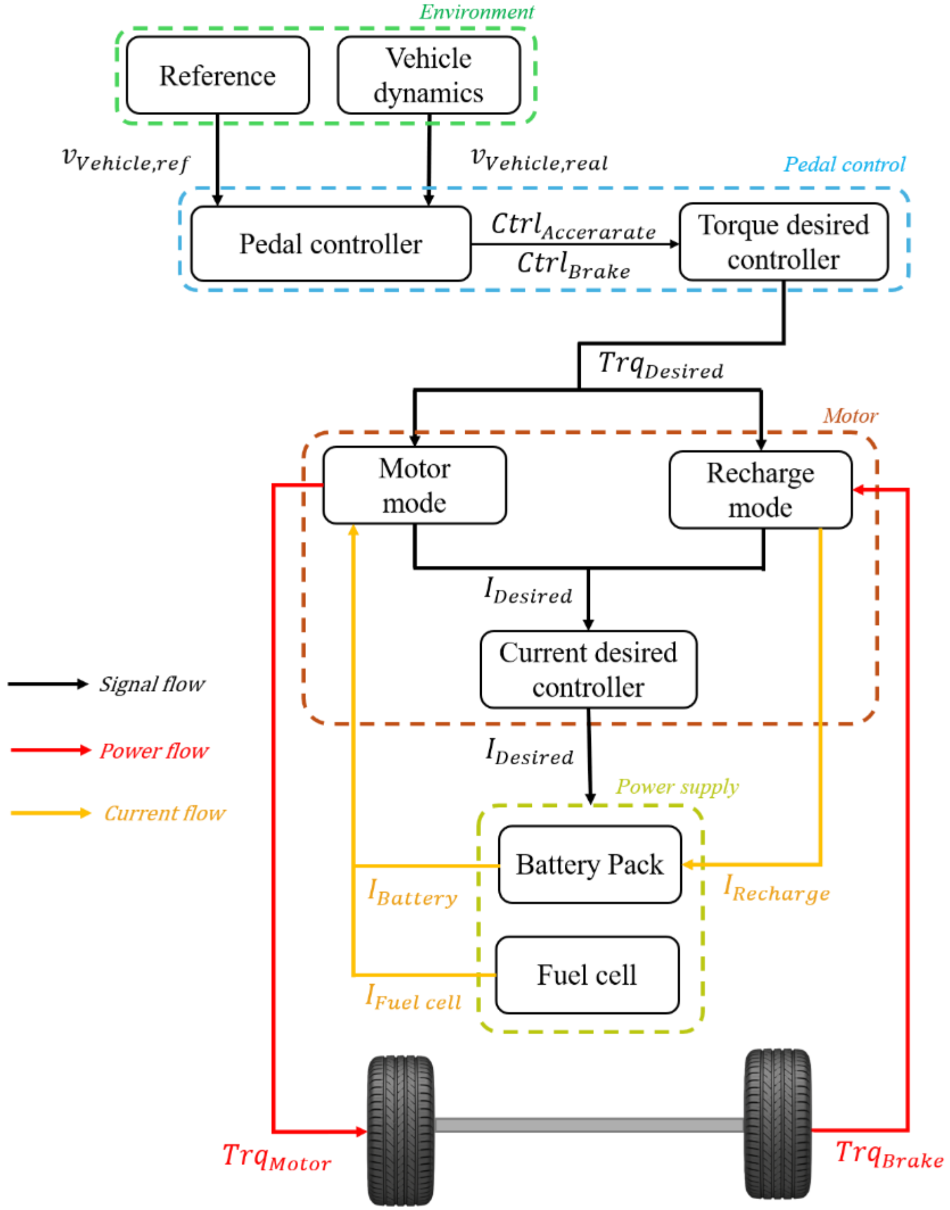

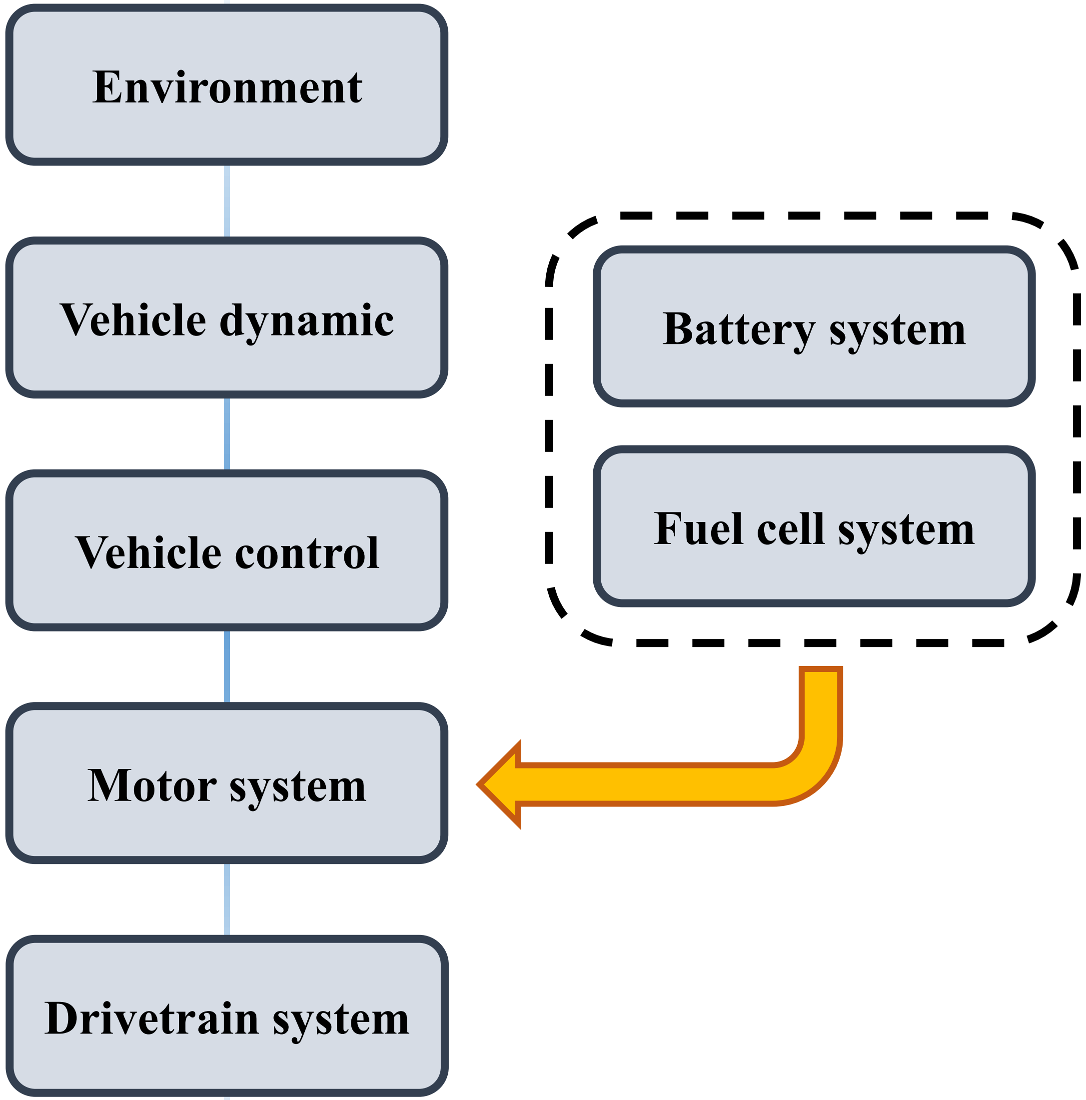

Fuel cell system

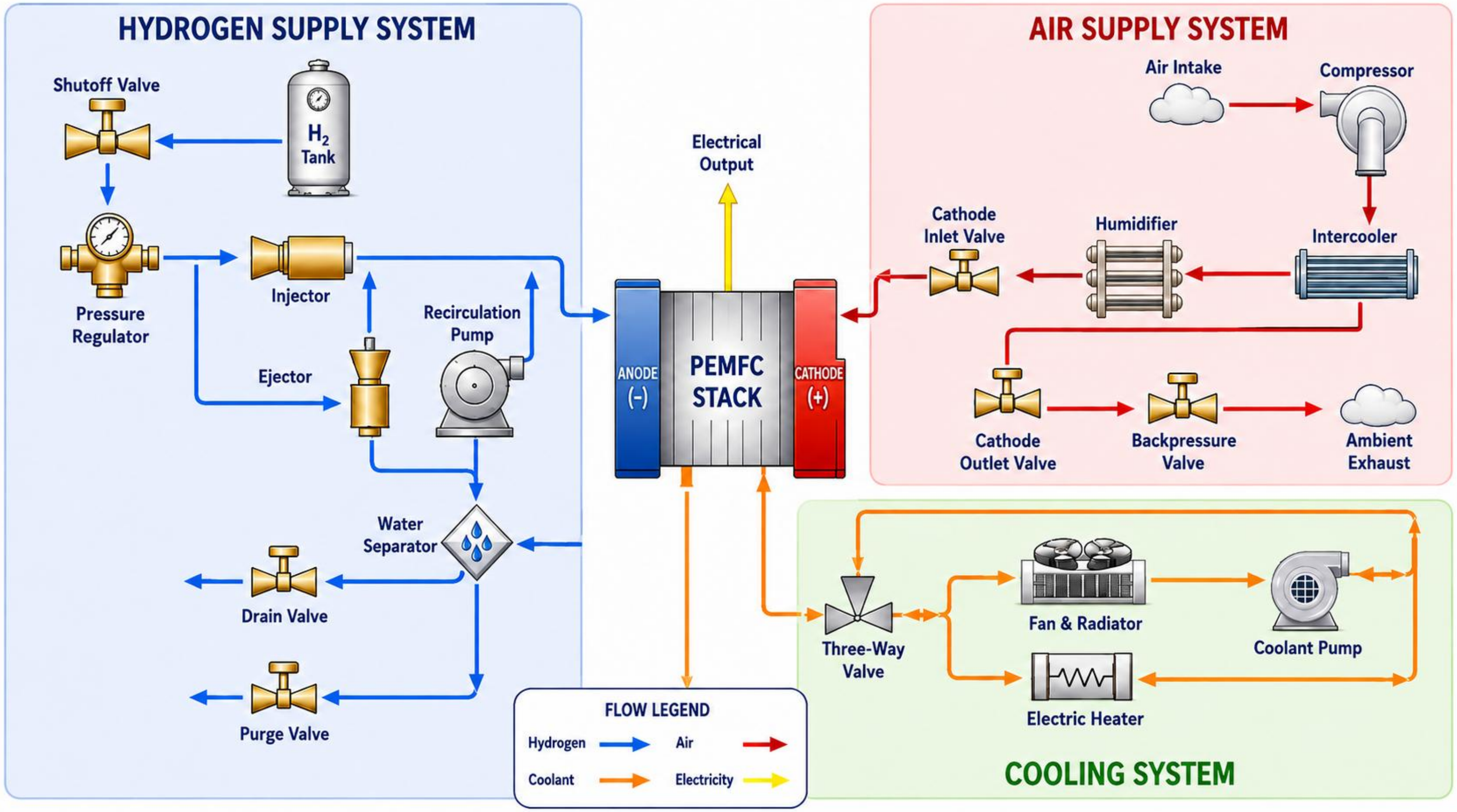

Anode inlet

Hydrogen Tank	Shutoff valve
Pressure regulator	Injector

Anode outlet

Purge valve	Drain valve

Anode Recirculation

Water separator	Recirculation pump	Ejector

Cathode inlet

Compressor	Intercooler	Isolation valve

Cathode outlet

Humidifier	Backpressure valve	Isolation valve

Cooling system

Coolant pump	Electric heater
Radiator	Fan

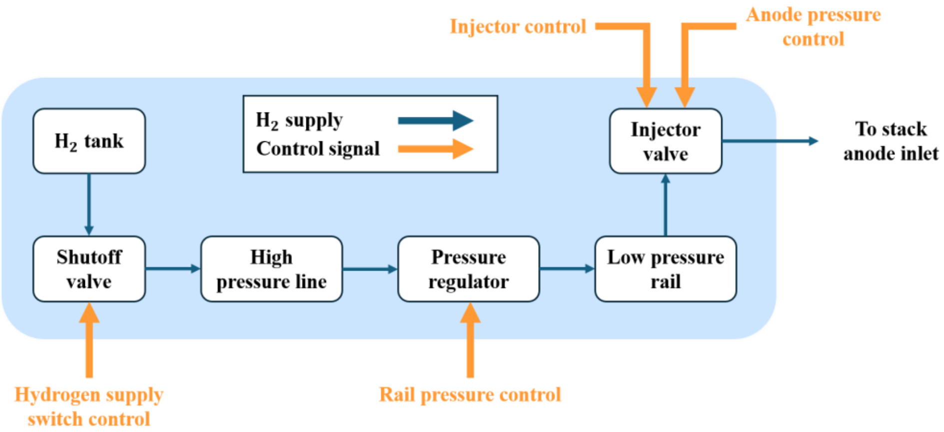

Hydrogen supply system

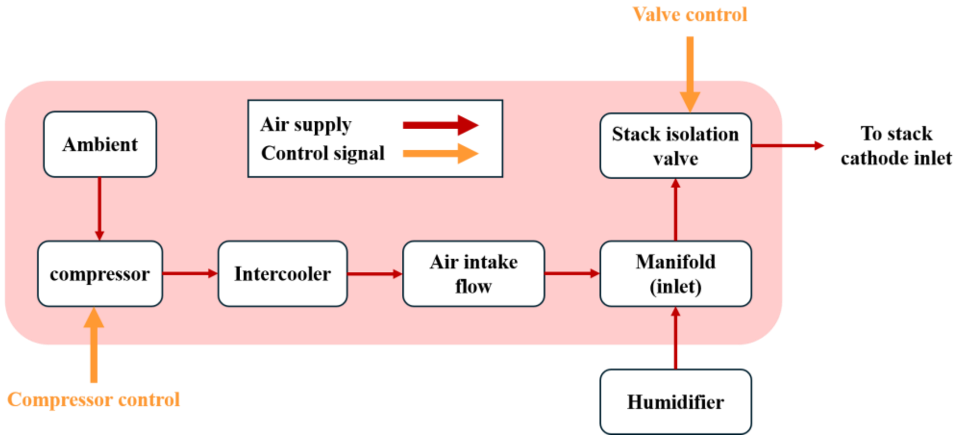

Air supply system

Compressor & Pump

Valve

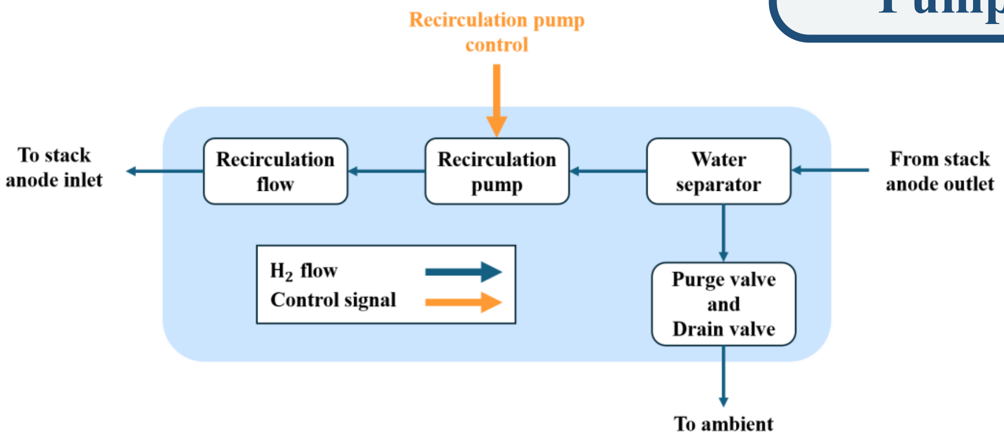

Hydrogen exhaust system

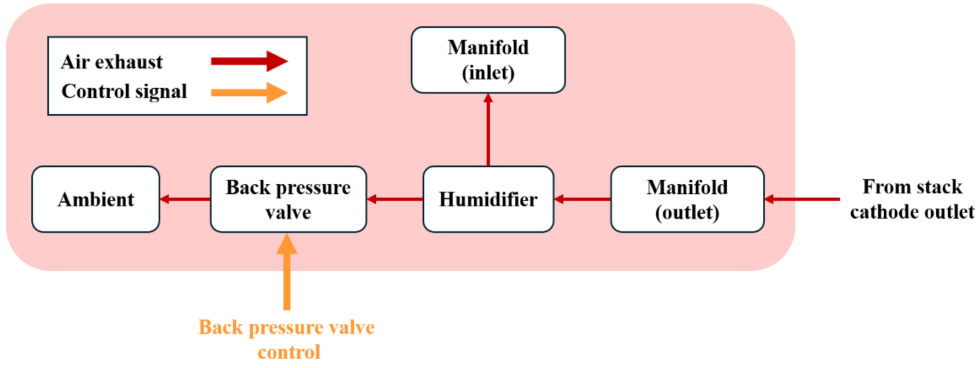

Air exhaust system

Vehicle Control

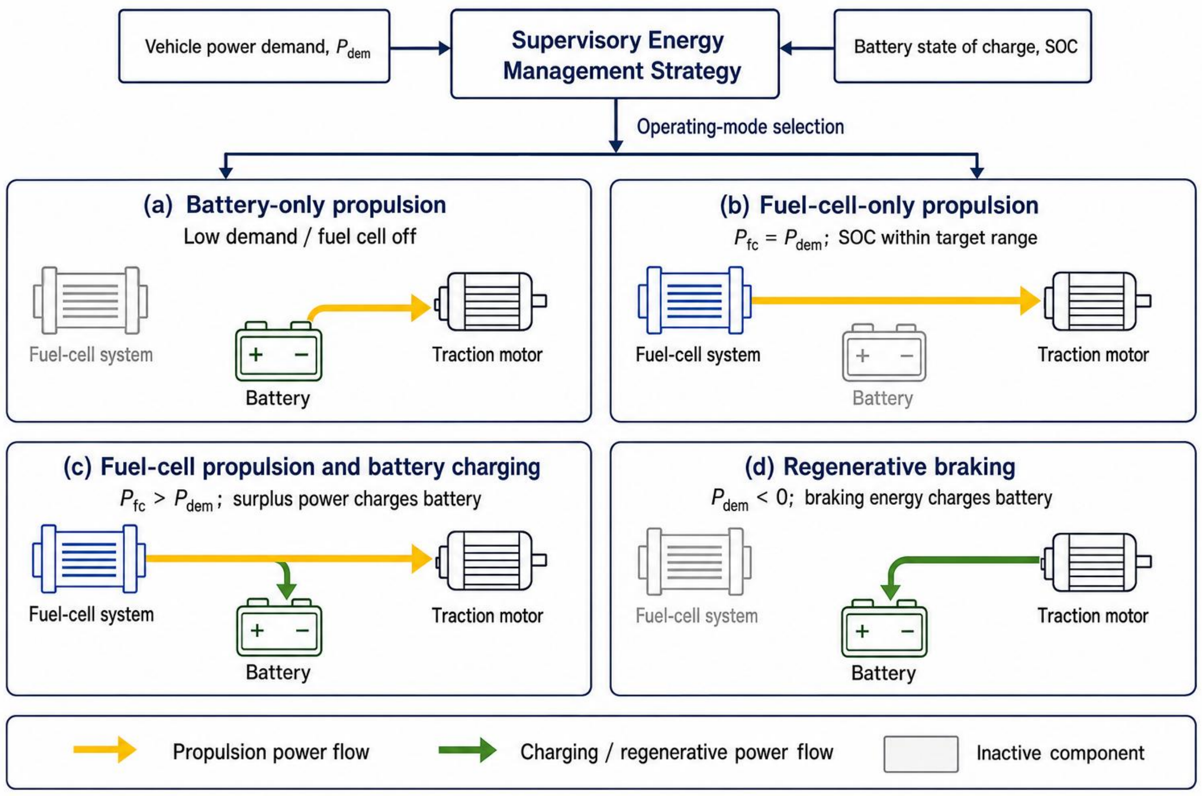

- **Start-up**: The lithium battery provides the initial traction power because the fuel cell requires a short period to establish stable electrochemical operation. This prevents delayed motor response during vehicle launch.
- **Acceleration**: As the traction power demand increases, the fuel cell and lithium battery operate together to supply the motor. The battery provides additional power to compensate for the slower dynamic response of the fuel cell.
- **Cruising**: Under relatively steady driving conditions, the fuel cell supplies most of the motor power. When the battery SOC is low and surplus fuel cell power is available, part of the energy can be used to recharge the battery.
- **Deceleration**: During braking or vehicle deceleration, the motor operates in regenerative mode. The recovered kinetic energy is converted into electrical energy and stored in the lithium battery for later use.

Environment

Manhattan Bus Cycle

MBC is a low-speed urban bus cycle with frequent stops and accelerations. It represents congested city traffic.

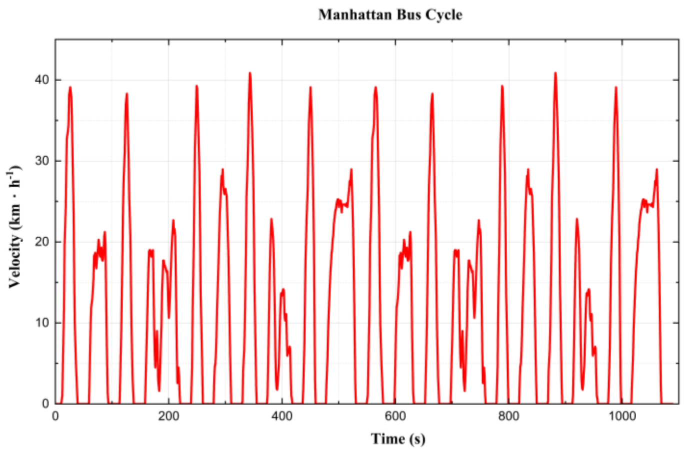

Travel time	1089 s	Average speed	11.0 km/h
Distance	3.33 km	Maximum speed	40.88 km/h

Braunschweig City Driving Cycle

BCDC is an urban bus cycle with repeated acceleration, deceleration, and stop-and-go operation. It covers a wider speed range than MBC.

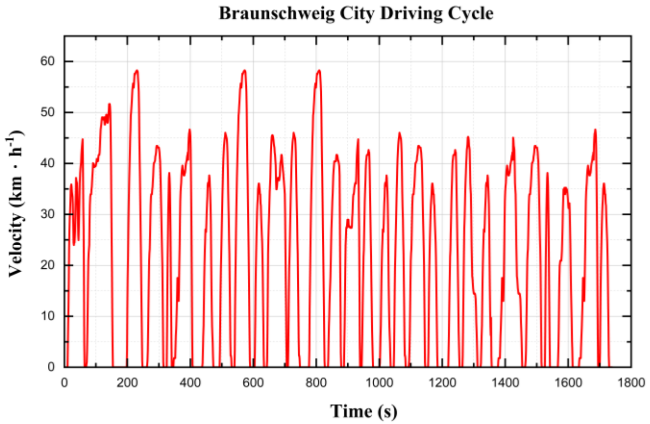

Travel time	1740 s	Average speed	22.53 km/h
Distance	10.88 km	Maximum speed	58.26 km/h

Orange County Bus Cycle

OCBC is a bus driving cycle with frequent speed variations and moderate-to-high speeds.

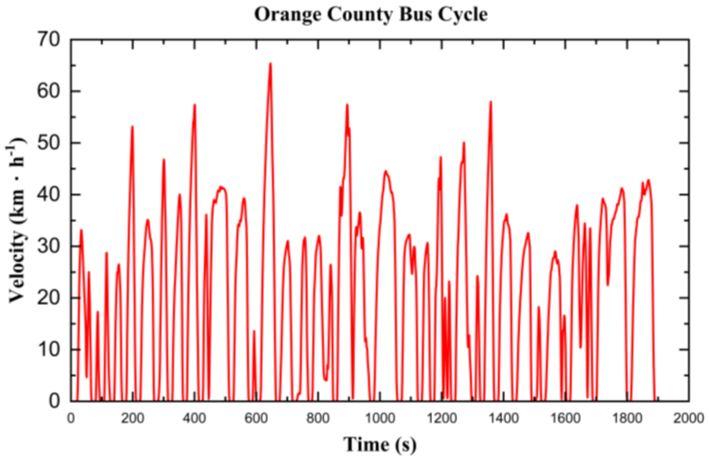

Travel time	1909 s	Average speed	19.31 km/h
Distance	10.53 km	Maximum speed	65.98 km/h

Heavy-Duty Urban Dynamometer Driving Schedule

HDUDDS is a heavy-duty urban driving cycle combining stop-and-go traffic with high-speed sections. It produces large variations in vehicle load and power demand.

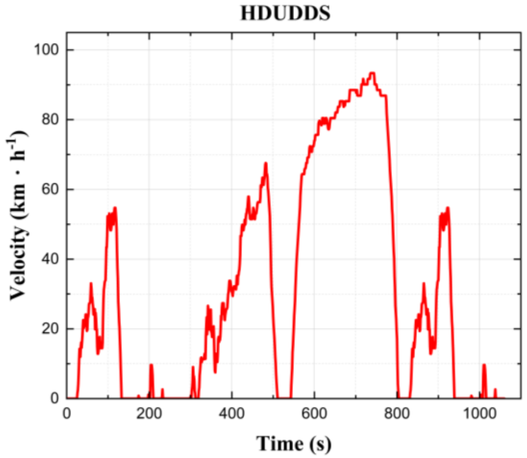

Travel time	1060 s	Average speed	30.35 km/h
Distance	8.93 km	Maximum speed	93.34 km/h

Surrogate Model (Agent model)

- Training data for the surrogate models were collected using the dSPACE SCALEXIO real-time platform. Stepwise fan and pump commands were applied across their operating ranges, while the corresponding coolant temperatures and system responses were recorded through ControlDesk. The measured input–output data were subsequently used for system identification and model validation.

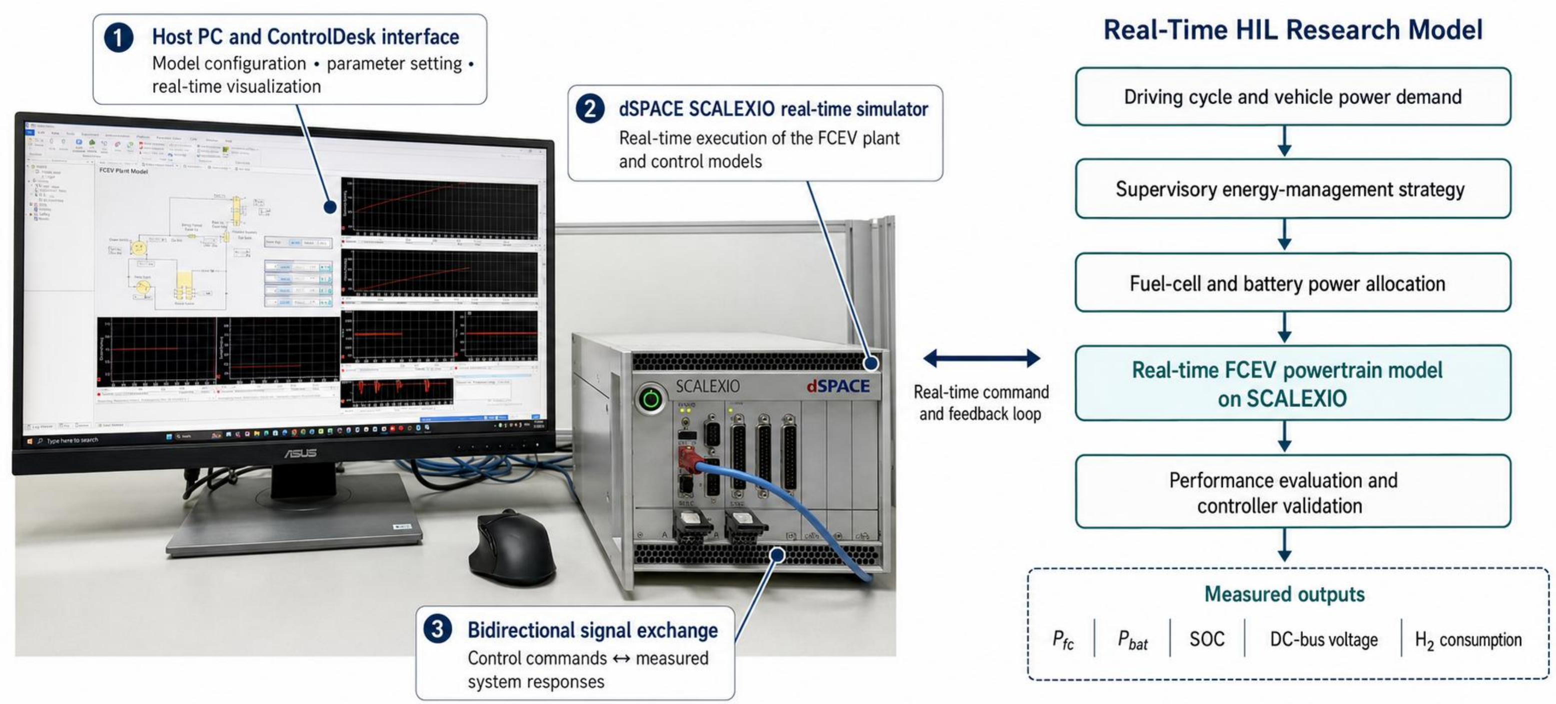

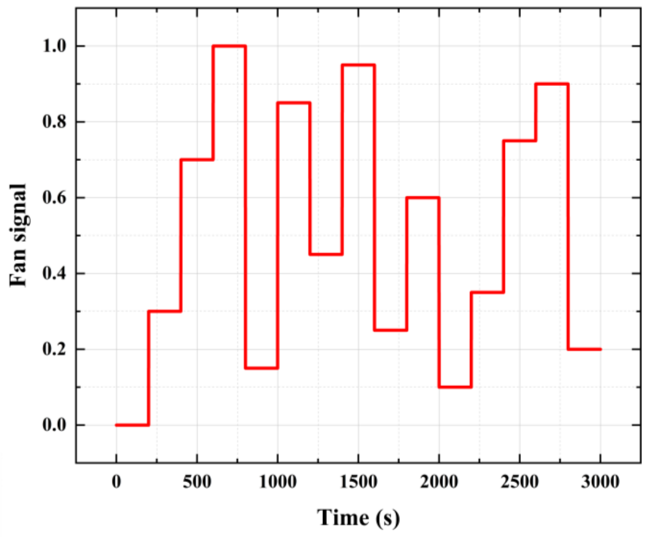

Fan Excitation Signal for Data Collection

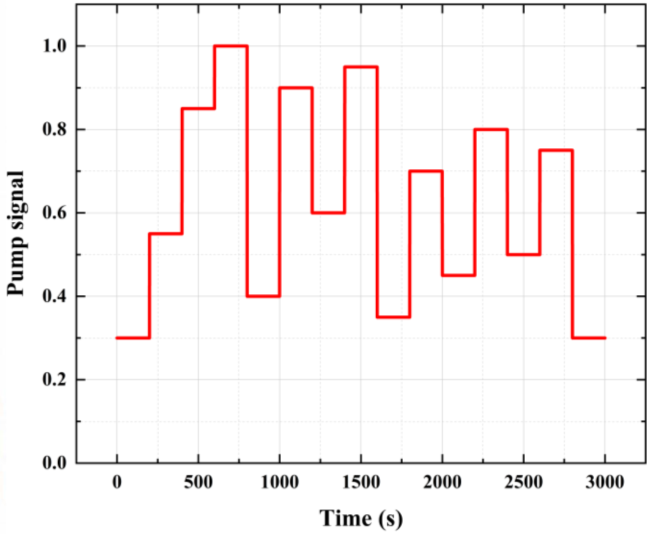

Pump Excitation Signal for Data Collection

Surrogate model

- System identification is used to construct a low-order surrogate model from input – output data, reducing the computational cost of controller optimization while preserving the dominant thermal dynamics.

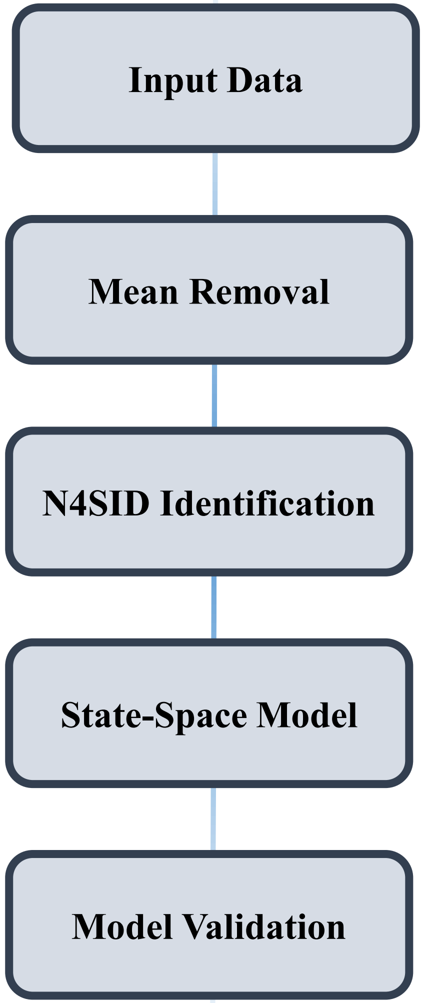

Key equation

Identified State-Space Model

- $x(k+1) = Ax(k) + Bu(k) + Ke(k)$
- $y(k) = Cx(k) + Du(k) + e(k)$

N4SID Identification Relation

- $Y_f = \Gamma_f X_k + H_f U_f + G_f E_f$

Model Accuracy Evaluation

- $fit = 100\left(1 - \frac{\|\hat{y} - y\|}{\|y - mean(y)\|}\right)$

Model I/O

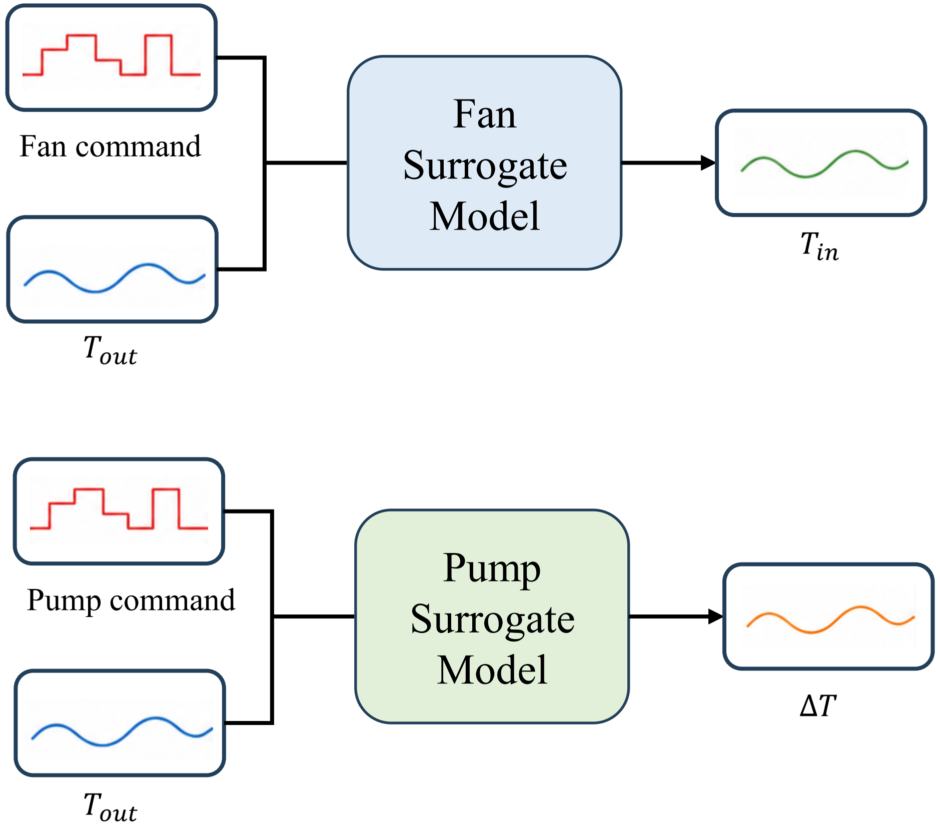

Sparrow Search Algorithm (SSA)

- **Producer**

$$X_{i,j}^{t+1} = \begin{cases} X_{i,j}^{t} \cdot \exp\left(-\frac{i}{\alpha \cdot iter_{max}}\right), R_2 < ST \\ X_{i,j}^{t} + Q \cdot L, R_2 \geq ST \end{cases}$$

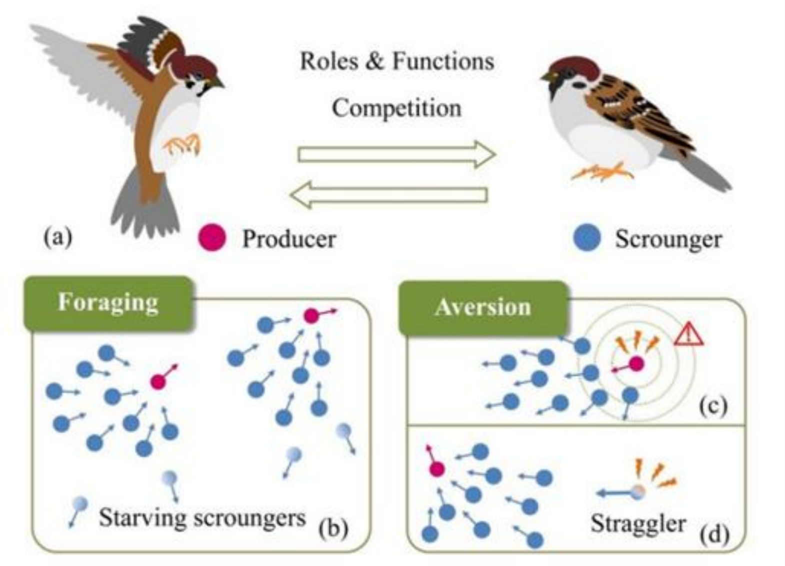

- **Scrounger**

$$X_{i,j}^{t+1} = \begin{cases} Q \cdot \exp\left(-\frac{X_{worst}^{t} - X_{i,j}^{t}}{i^2}\right), i > \frac{n}{2} \\ X_P^{t+1} + \left|X_{i,j}^{t} - X_P^{t+1}\right| \cdot A^{+} \cdot L, otherwise \end{cases}$$

- **Aware Sparrows**

$$X_{i,j}^{t+1} = \begin{cases} Q \cdot \exp\left(-\frac{X_{worst}^{t} - X_{i,j}^{t}}{i^2}\right), i > \frac{n}{2} \\ X_P^{t+1} + \left|X_{i,j}^{t} - X_P^{t+1}\right| \cdot A^{+} \cdot L, otherwise \end{cases}$$

Sparrow Search Algorithm (SSA)

- **Initialize Candidate PI Gains**
- **Simulate Surrogate Model**
- **Evaluate Objective Function**
- **Update Sparrow Positions**
- **Check Convergence and Output Optimal Gains**

$$J_{fan} = J_{T,high} + J_{T,low} + J_{u} + J_{\Delta u} + J_{sat} + J_{ss}$$

Temperature Tracking Performance ($J_{T,high} + J_{T,low}$; $J_{\Delta T,high} + J_{\Delta T,low}$)

Control Effort and Stability ($J_{u} + J_{\Delta u} + J_{sat} + J_{ss}$)

$$J_{pump} = J_{\Delta T,high} + J_{\Delta T,low} + J_{u} + J_{\Delta u} + J_{sat} + J_{ss}$$

Number of sparrows	50
Maximum iteration	70
Search dimension	2
Final selection criterion	Minimum fitness value
Initial PI gains	K_p: 0.05 K_i: 0.005
Search range of PI gains	$\mathrm{K_p} \in [0, 0.2]$ $\mathrm{K_i} \in [0, 0.01]$

Fuzzy Control

- **Vehicle Speed Input**
- **Membership Calculation**
- **Fuzzy Rule Evaluation**
- **PI Gain Scheduling**
- **Fan and Pump PI Control**

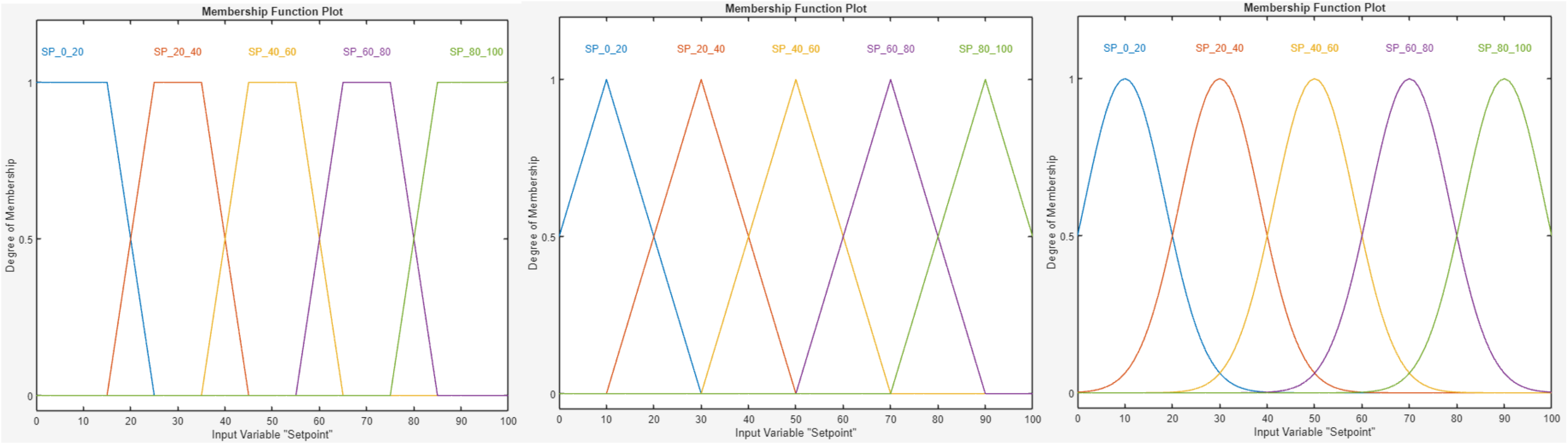

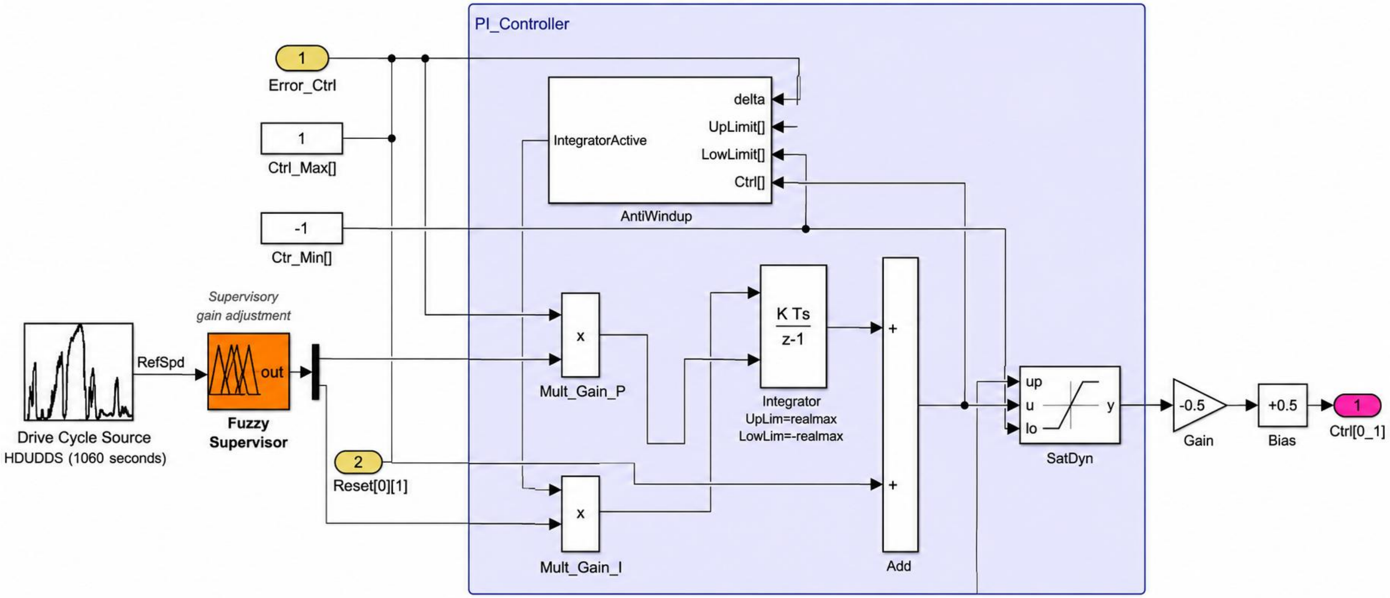

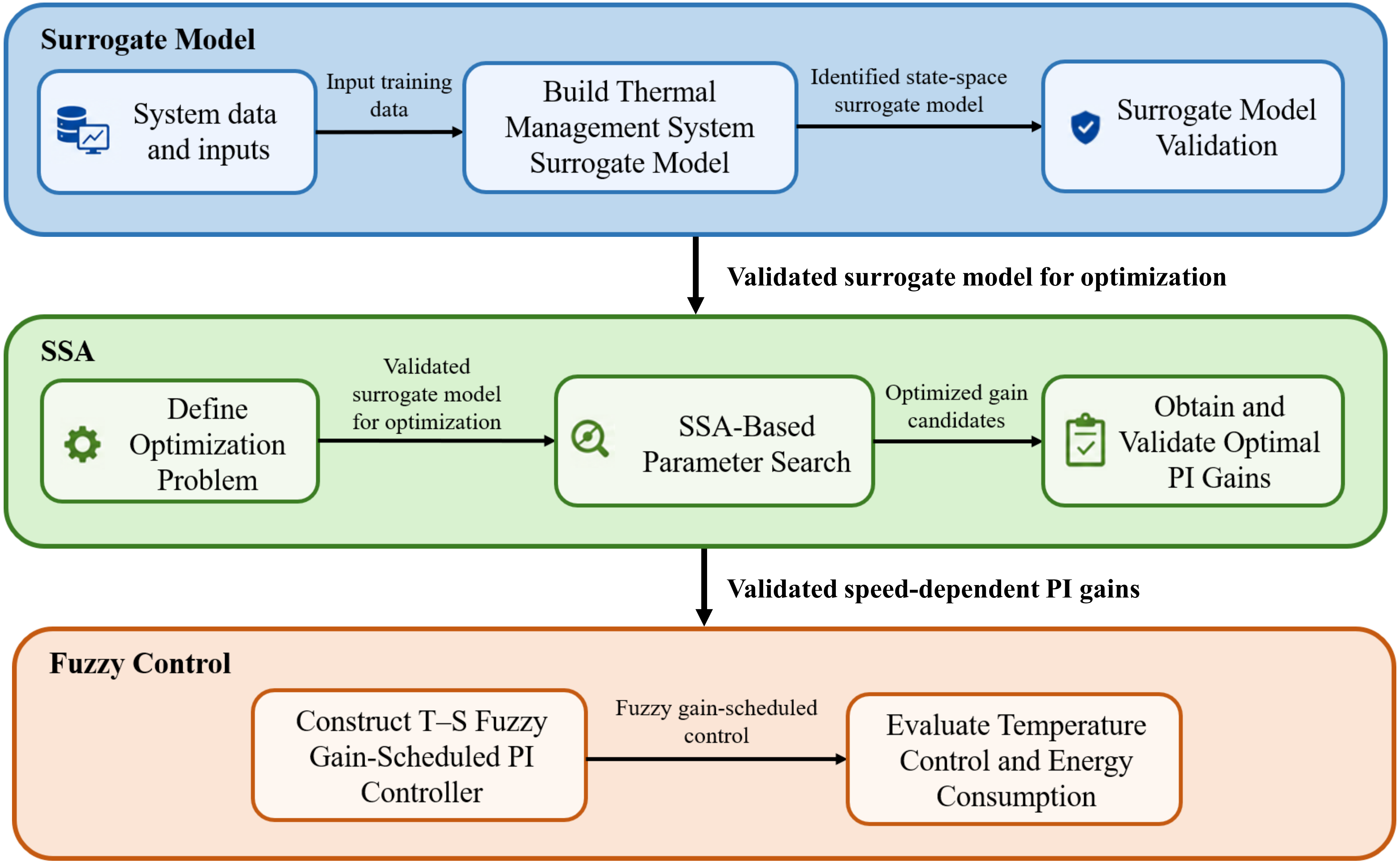
Surrogate Model
System data and inputs
Input training data
Build Thermal Management System Surrogate Model
Identified state-space surrogate model
Surrogate Model Validation
Validated surrogate model for optimization
SSA
Define Optimization Problem
Validated surrogate model for optimization
SSA-Based Parameter Search
Optimized gain candidates
Obtain and Validate Optimal PI Gains
Validated speed-dependent PI gains
Fuzzy Control
Construct T–S Fuzzy Gain-Scheduled PI Controller
Fuzzy gain-scheduled control
Evaluate Temperature Control and Energy Consumption

Test Cycle Verification

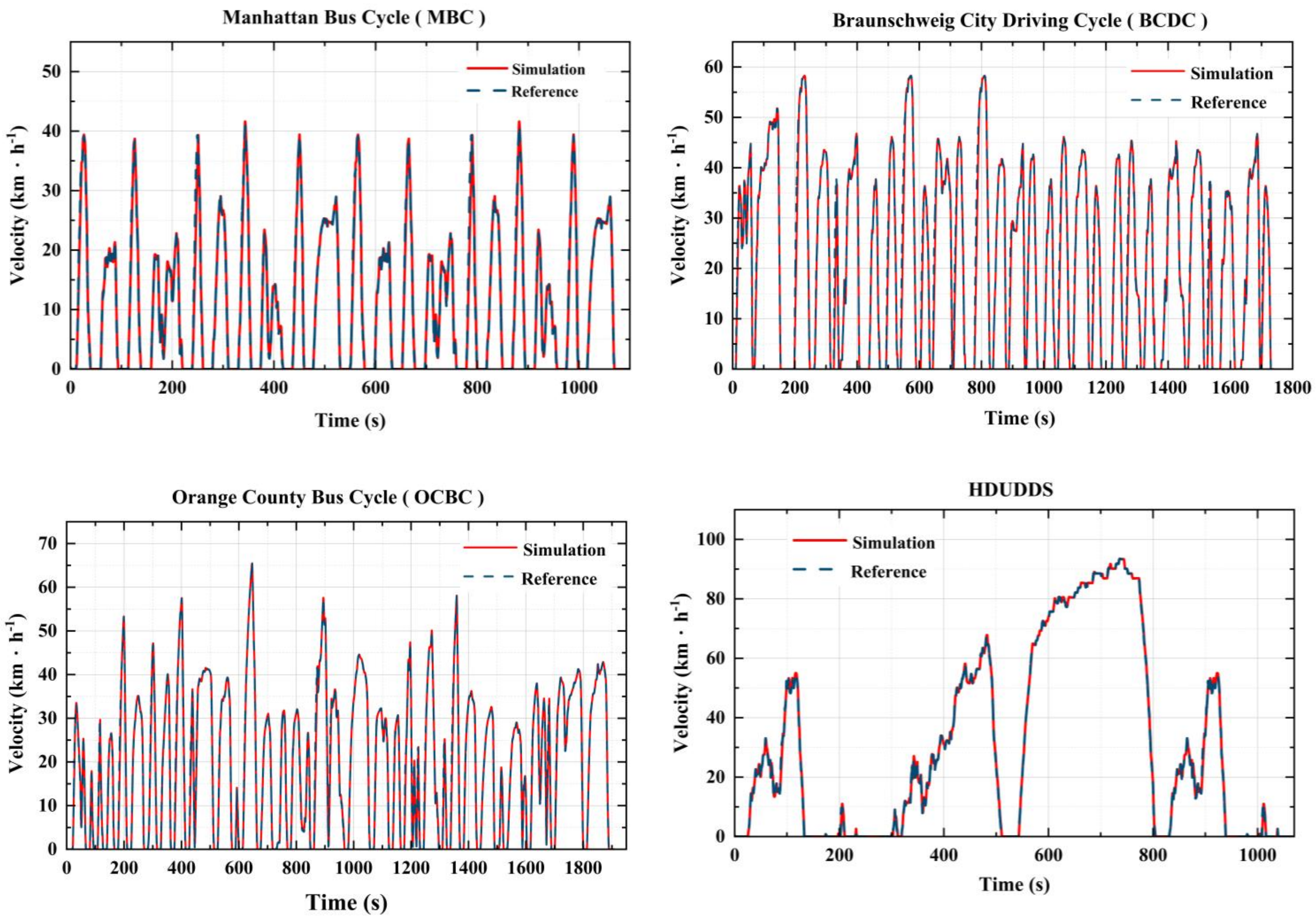

The four driving cycles provide a comprehensive evaluation of the vehicle model under different speed ranges and transient conditions. The simulated vehicle speed closely follows the reference profile in MBC, BCDC, OCBC, and HDUDDS [7] , including frequent stop-and-go operation and high-speed variations. These results confirm the model ability to accurately reproduce vehicle speed dynamics under various driving conditions.

[7] A. Łebkowski, Studies of Energy Consumption by a City Bus Powered by a Hybrid Energy Storage System in Variable Road Conditions. Energies 12(5) (2019) 951.

System Verification

The fan and pump power models were validated under a total fuel cell output of 180 kW. The simulated pump and fan powers were 1.11 and 12.57 kW, with relative errors of 2.70% and 0.55%, confirming good agreement with the reference values.

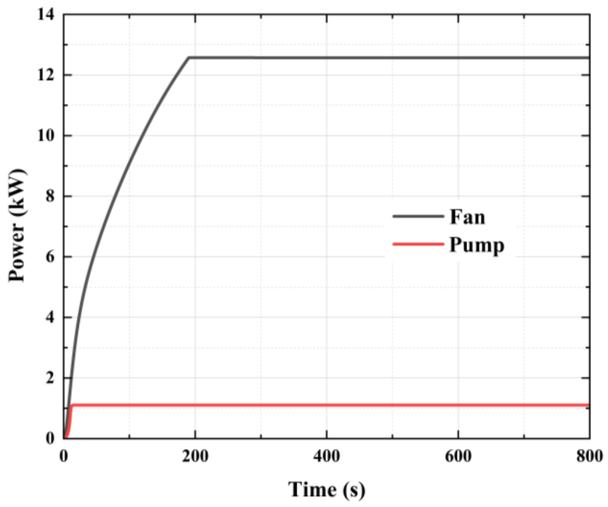

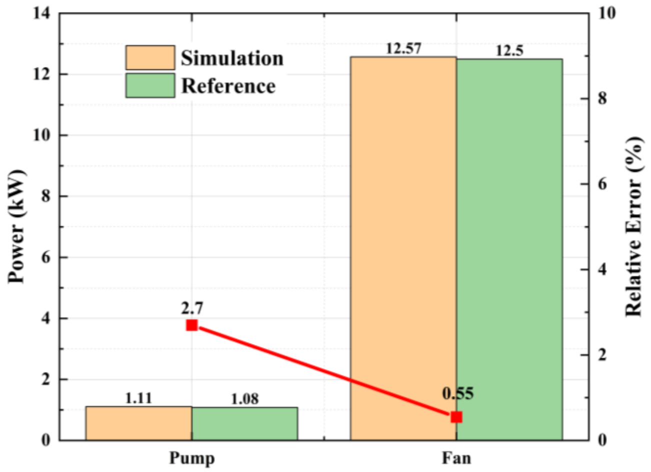

The motor model was validated using four driving cycles. The operating points remained within the reference torque–speed envelope. Relative errors at selected speeds ranged from 0.20% to 3.20%, confirming good agreement with the reference data.

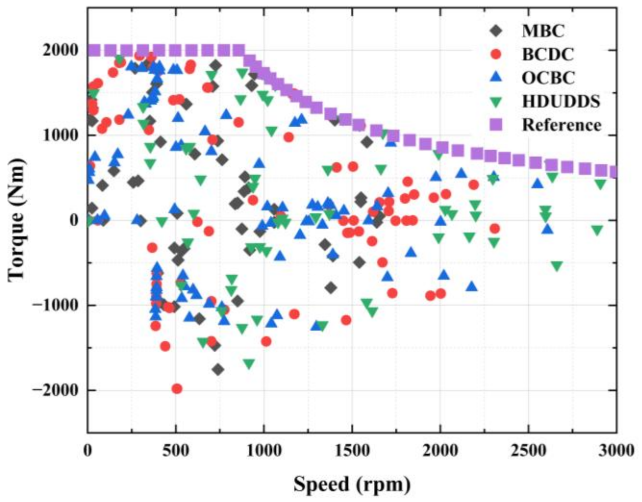

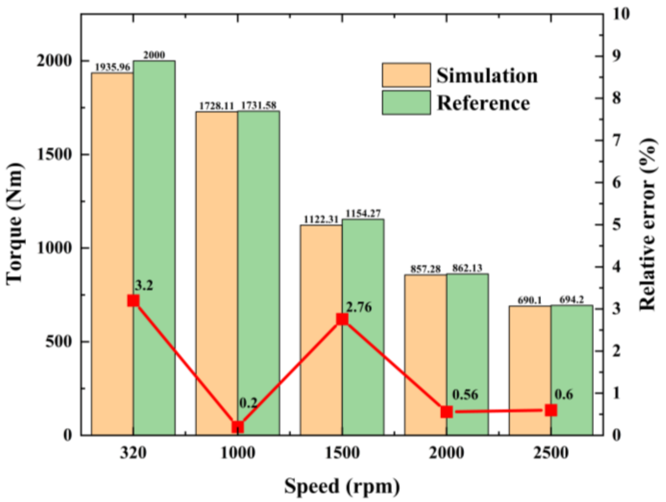

[8] Y. Kim, J. Kim, and K. Min, Analysis of power consumption on BOP system in a fuel cell electric bus according to the fuel cell load range. International Journal of Automotive Technology 25(4) (2024) 701-715.

[9] A. Ritari, J. Vepsäläinen, K. Kivekäs, K. Tammi, and H. Laitinen, Energy Consumption and Lifecycle Cost Analysis of Electric City Buses with Multispeed Gearboxes. Energies 13(8) (2020) 2117.

Vehicle System Performance

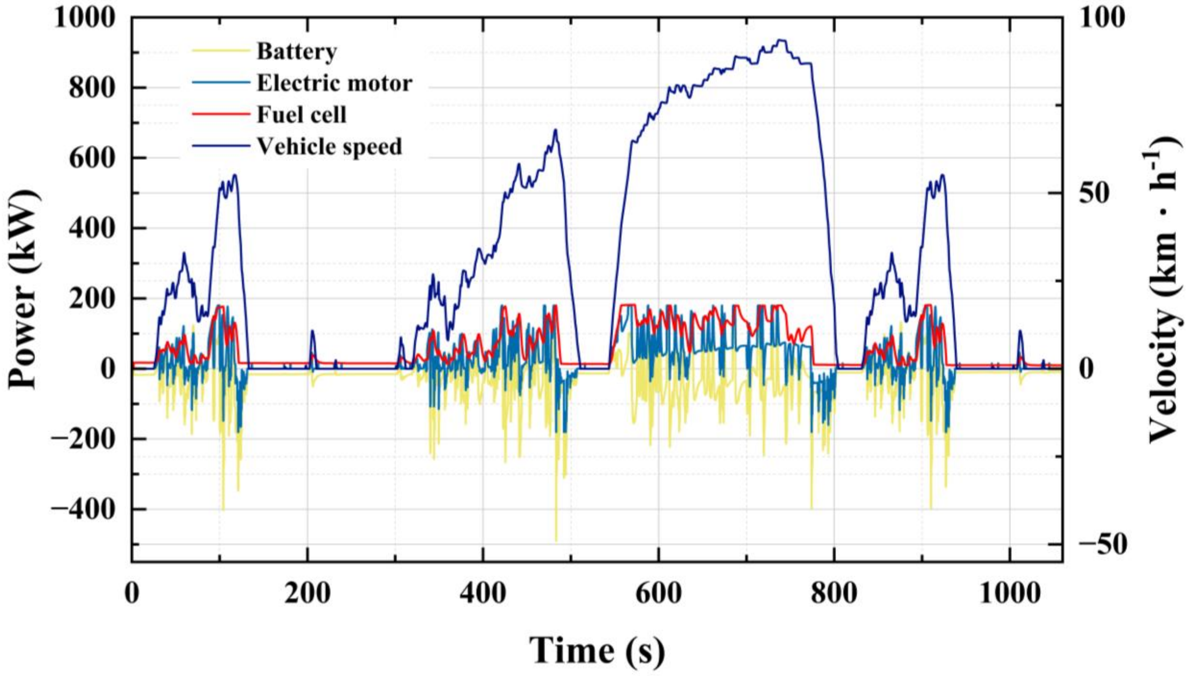

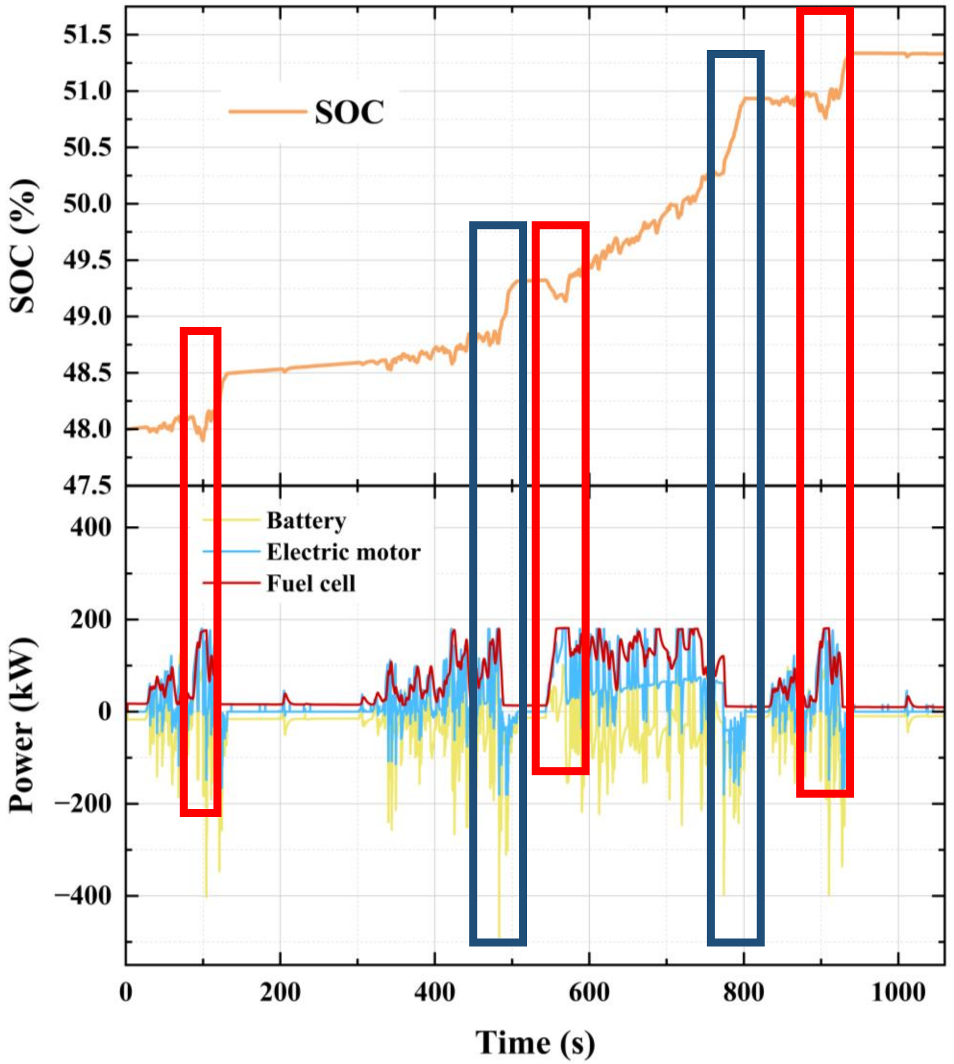

- The traction power demand varies with vehicle speed. The fuel cell provides the primary power, while the battery supports transient load changes and absorbs regenerative braking energy during deceleration.
- The battery SOC increases from approximately 48.0% to 51.3%, indicating that regenerative braking energy and surplus fuel cell power are stored in the battery. The fuel cell and battery jointly satisfy the motor power demand under dynamic driving conditions.

PI Controller Optimization

Second , third , and fourth-order state-space models were evaluated using separate estimation and validation datasets. The estimation fits exceeded 93%, while the validation fits ranged from 83.34% to 86.59%. Since increasing the model order did not consistently improve validation accuracy, the second-order model was selected to balance prediction performance, generalization capability, and computational efficiency.

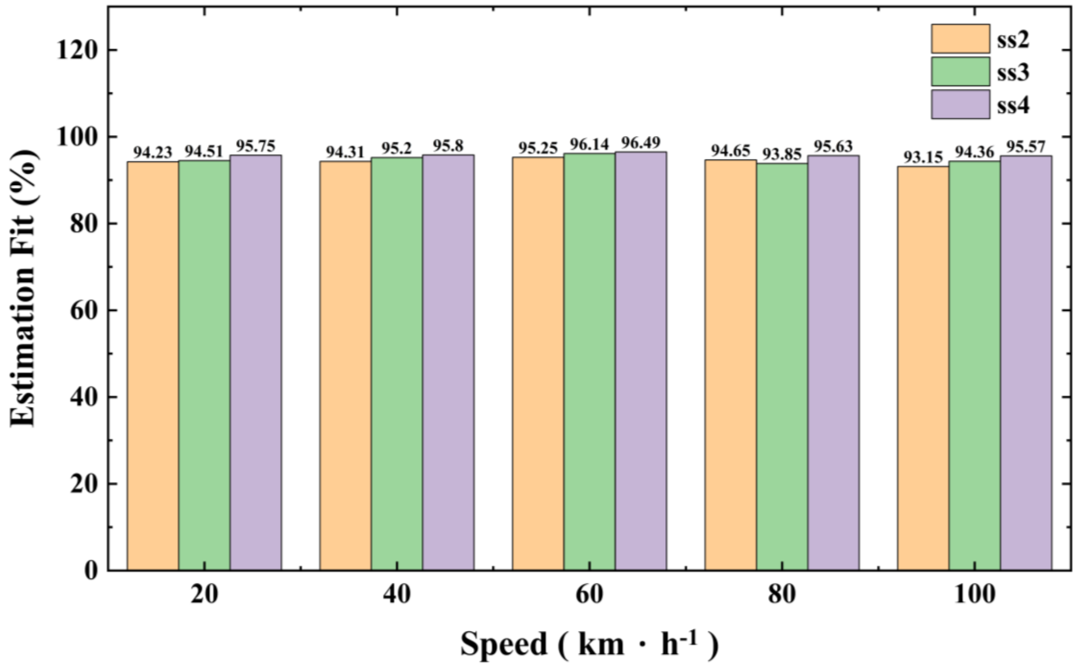

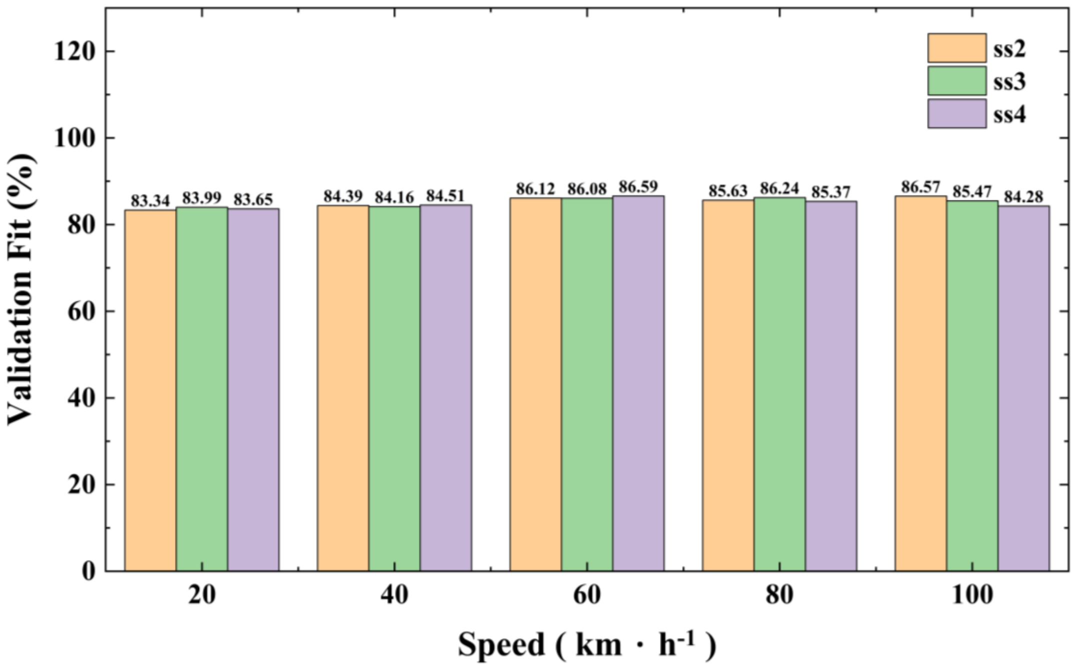

B Sparrow Search Algorithm (SSA)Convergence at Different Vehicle Speeds

The objective function decreased rapidly during the early iterations and gradually converged to a stable value at all tested vehicle speeds. Most cases reached convergence within approximately 10~30 iterations , indicating that SSA can efficiently and consistently identify suitable PI controller parameters.

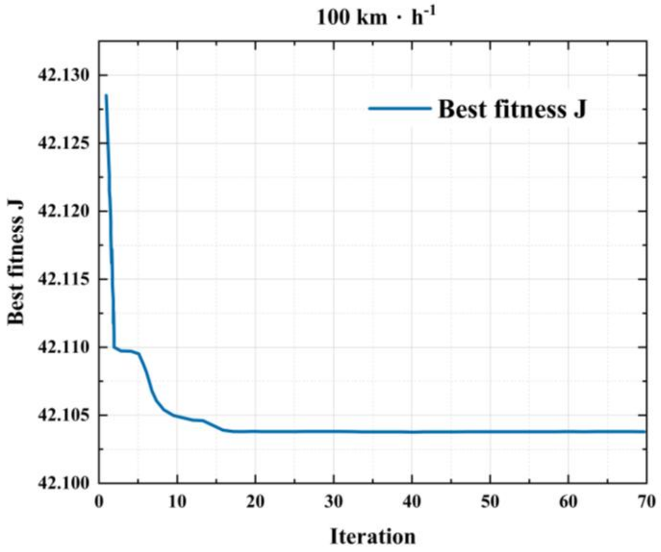

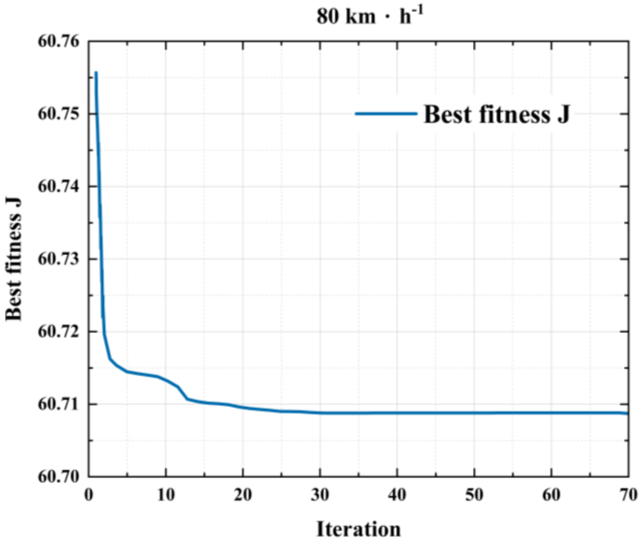

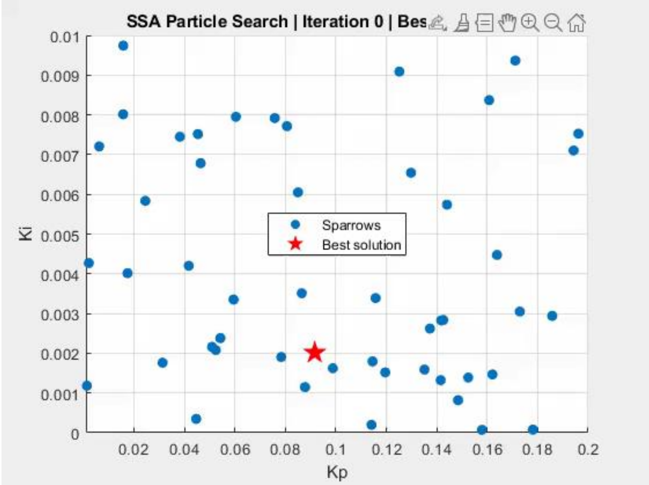

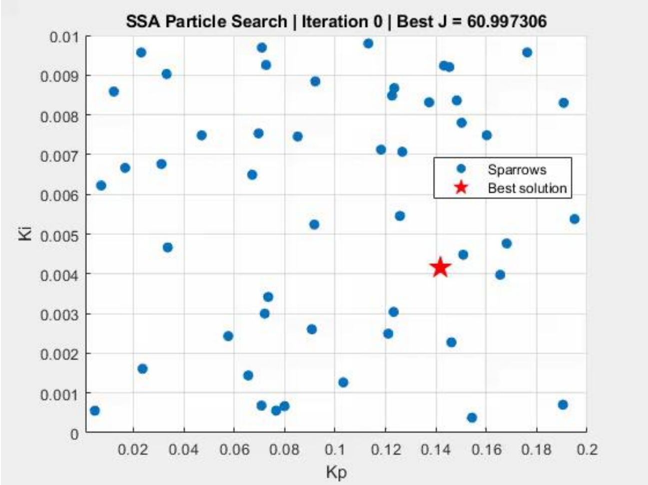

B Sparrow Search Algorithm (SSA) Convergence at Different Vehicle Speeds

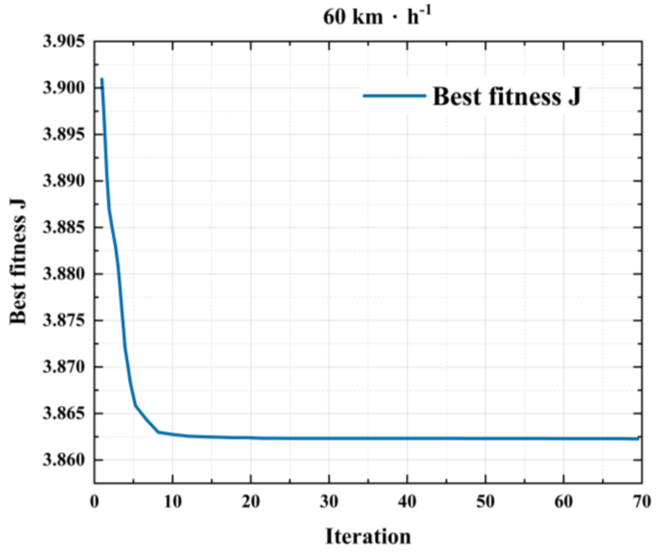

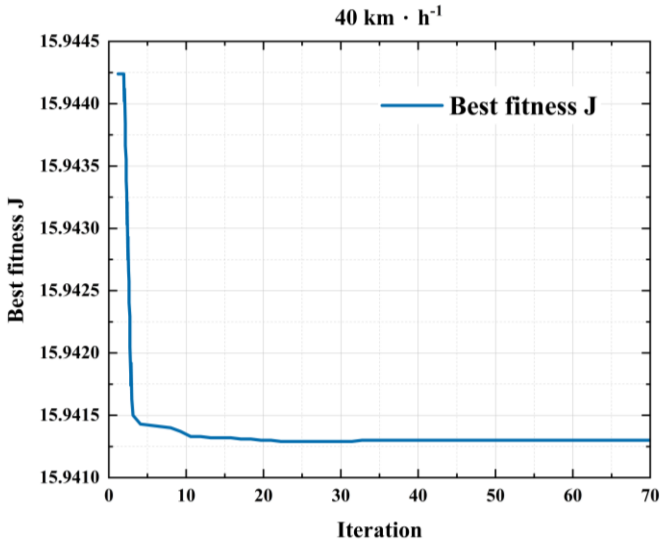

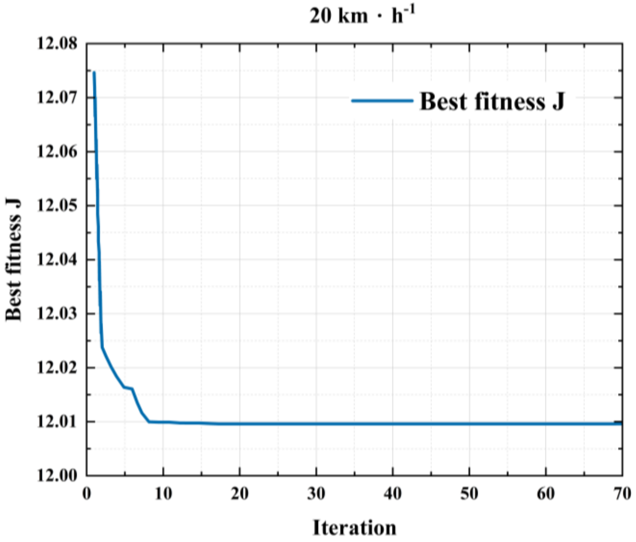

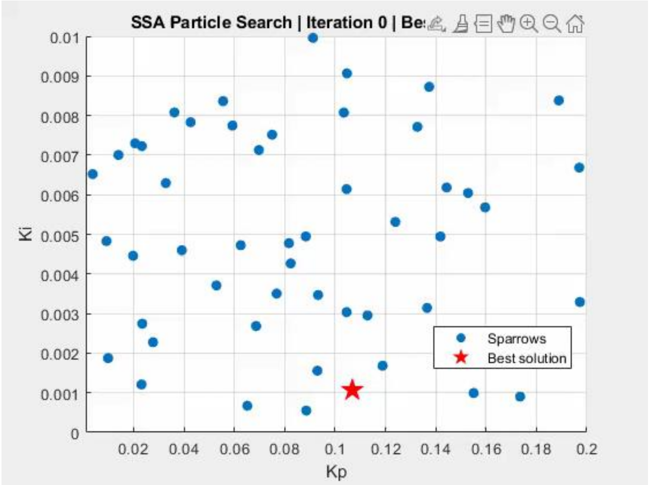

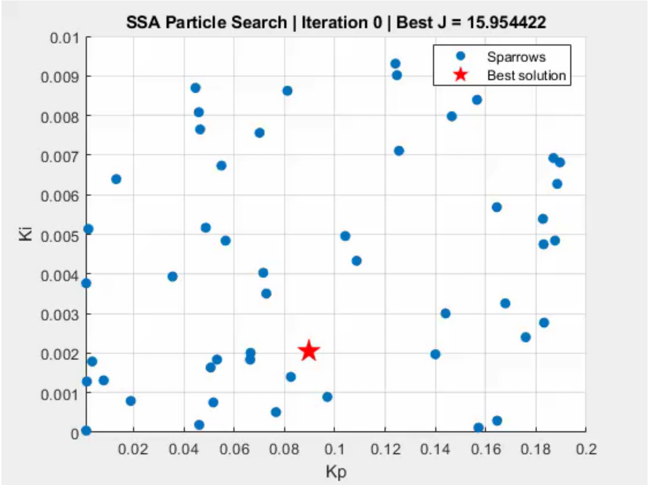

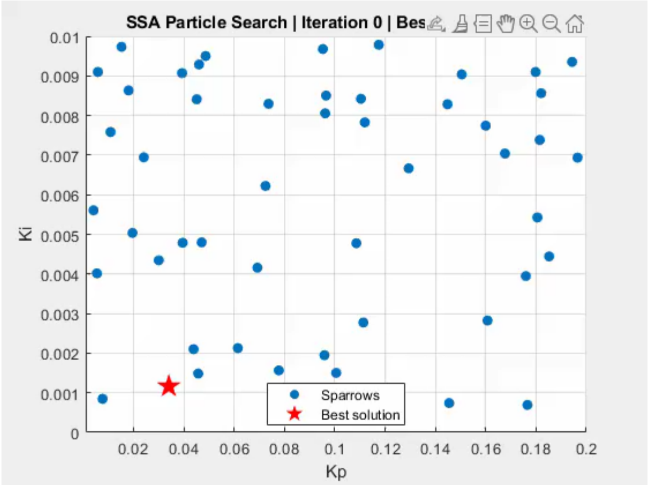

C Speed-Scheduled Optimization Test Conditions

A multi-speed test profile was designed to evaluate the optimized PI controller under different thermal-load conditions. After an initial 200 s acceleration period, each speed was maintained for 150 s to ensure that the thermal response approached a stable operating condition.

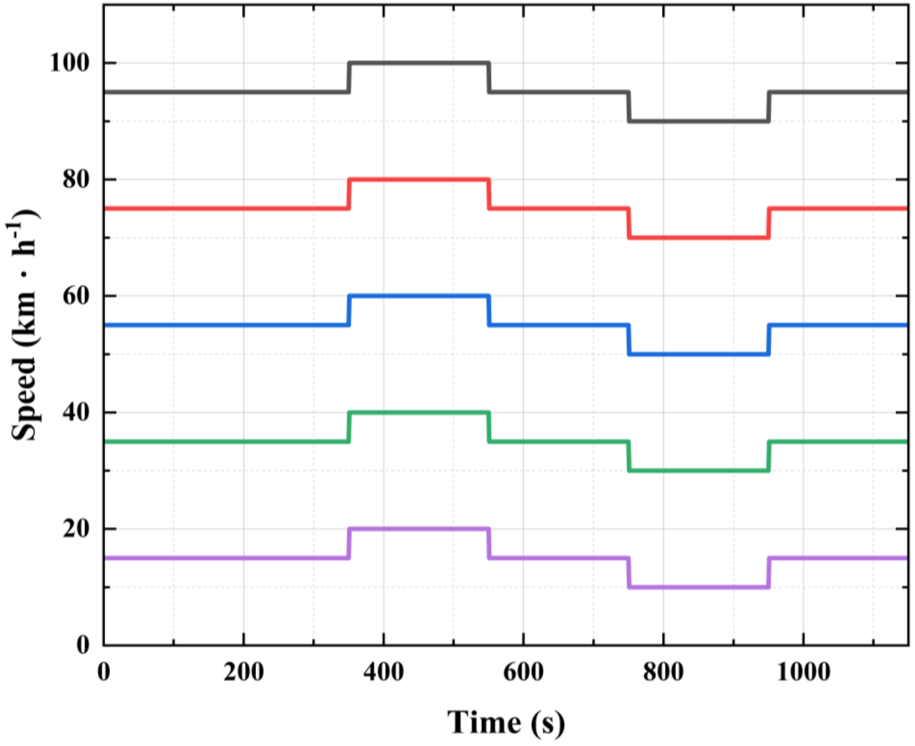

Test speeds	100, 80, 60, 40, and 20 km/h
Initial acceleration period	200 s
Duration of each speed segment	150 s
Comparison	Original PI vs. SSA-Optimized PI

D Control Response and Energy Consumption at 100 km/h

- The pump is controlled by a feedforward lookup table, so its command remains nearly unchanged after optimization.
- The optimized fan PI controller reduces control oscillation and peak duration.
- Unnecessary fan operation is reduced, resulting in a 5.11% decrease in fan energy consumption.

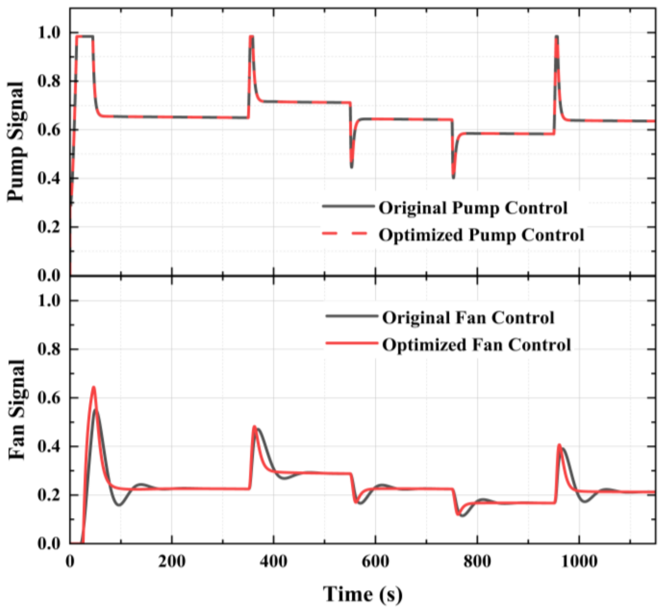

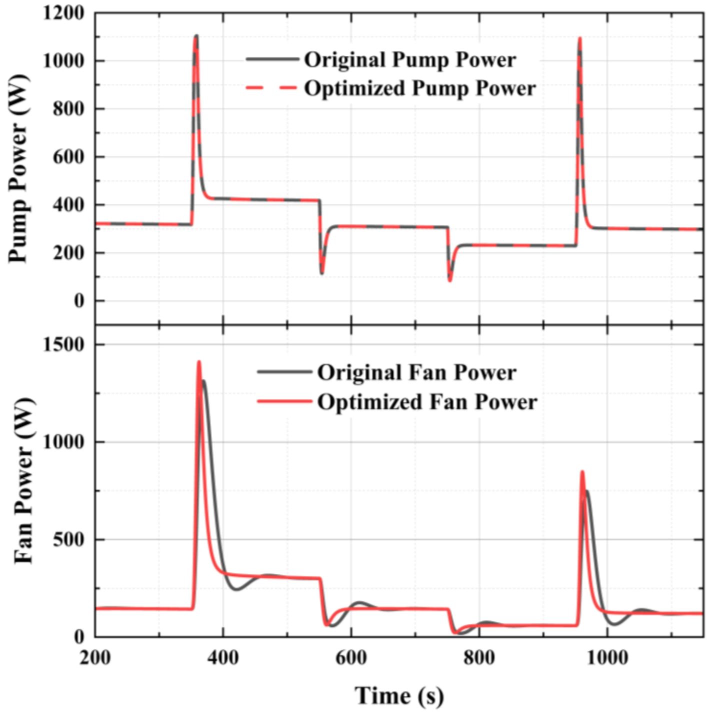

Control Strategy	Fan Energy Consumption (Wh)	Energy Saving Rtae (%)
Original PI	50.34	–
Optimized PI	47.20	5.11 %

Comparison of Thermal Management Strategies

- **FFP–OPI**：

Feedforward Pump + Original PI Fan Control

- **FFP–SFPI**：

Feedforward Pump + SSA-Optimized Fuzzy PI Fan Control

- **SOPP–SFPI**：

Optimized Pump PI + SSA-Optimized Fuzzy PI Fan Control

FFP–SFPI provides the best balance between temperature-tracking accuracy and auxiliary energy consumption.

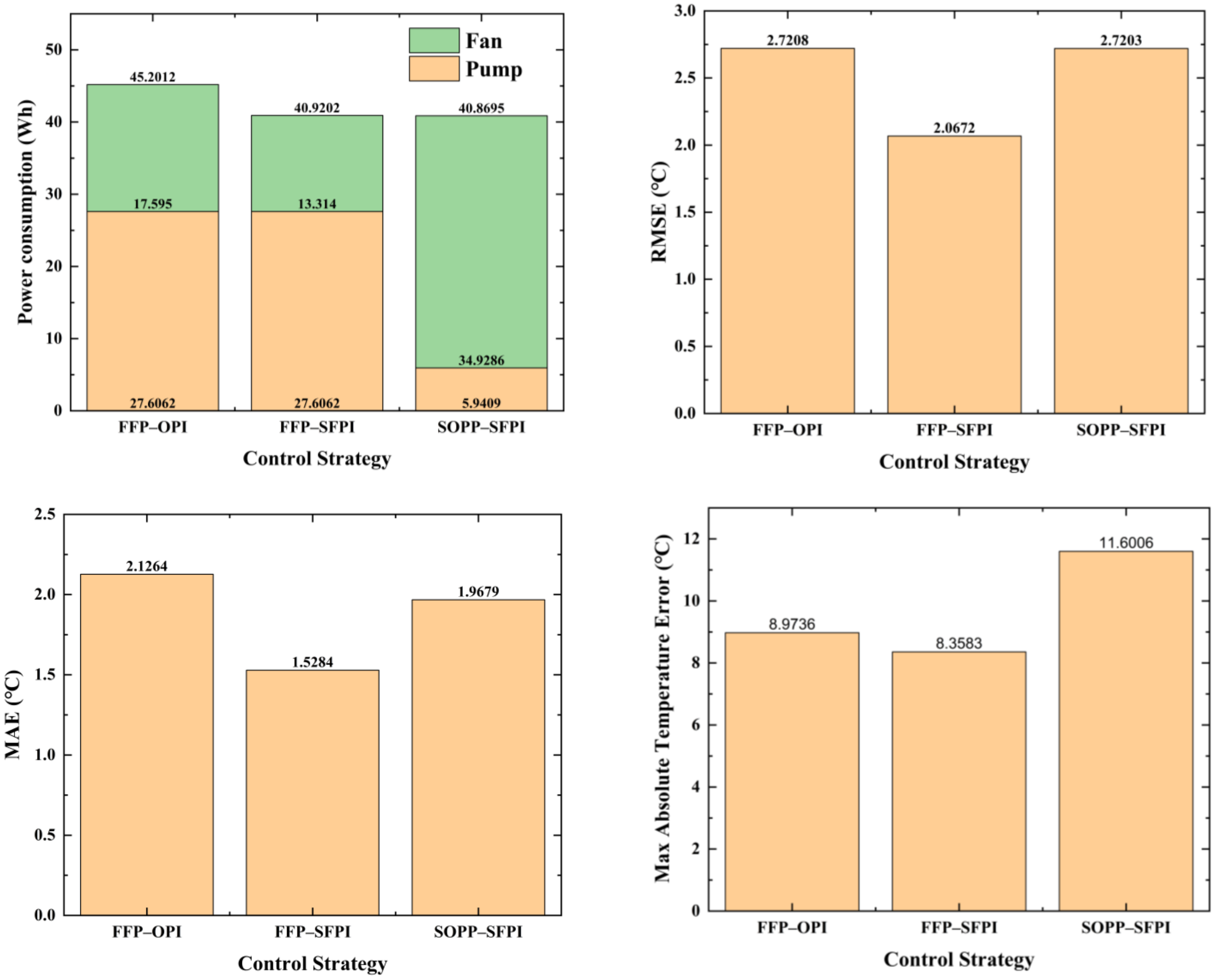

Research Highlights

Surrogate-Model-Based SSA Optimization with Fuzzy Gain-Scheduled PI Control
for Fuel Cell Bus Thermal Management

1. Research problem

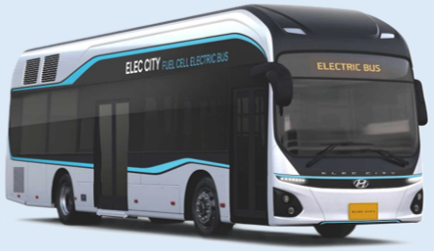

Fuel Cell Bus Thermal Management Challenge

- Thermal load varies with vehicle speed
- Fixed-gain PI control cannot adapt to all operating conditions

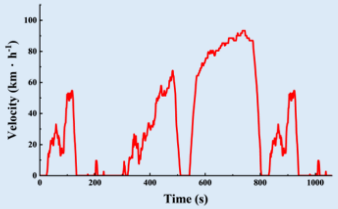

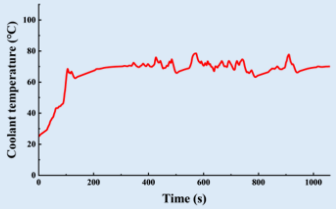

2. Research Methodology

1 dSPACE Data Collection

- Real-time control
- Data acquisition
- Fan, pump, and
- temperature signals

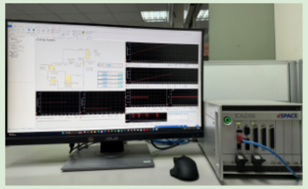

2 Surrogate Model Development

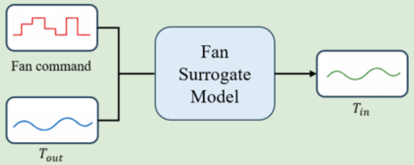

3 SSA Optimization of PI Parameters

Search Space (K_p, K_i)

- K_i
- K_p

4 Fuzzy Gain-Scheduled PI Control

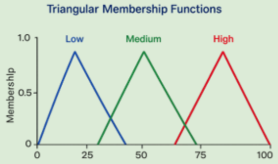

3. Performance evaluation

Control Strategy Comparison

- FFP–OPI : Feedforward Pump + Original PI Fan
- FFP–SFPI : Feedforward Pump + SSA-Optimized Fuzzy PI Fan
- SOPP–SFPI : SSA-Optimized Pump PI + SSA-Optimized Fuzzy PI Fan

Evaluation Metrics

- RMSE
- MAE
- Maximum Absolute Temperature Error
- Auxiliary Energy

4. Key outcomes

Best Strategy: FFP–SFPI

Total Auxiliary Energy	9.47% ↓
RMSE	24.02% ↓
MAE	28.12% ↓
Maximum Absolute Temperature Error	6.86% ↓

Our Team's Research Interests

Metal-Support Solid Oxide Fuel Cell (MS-SOFC)

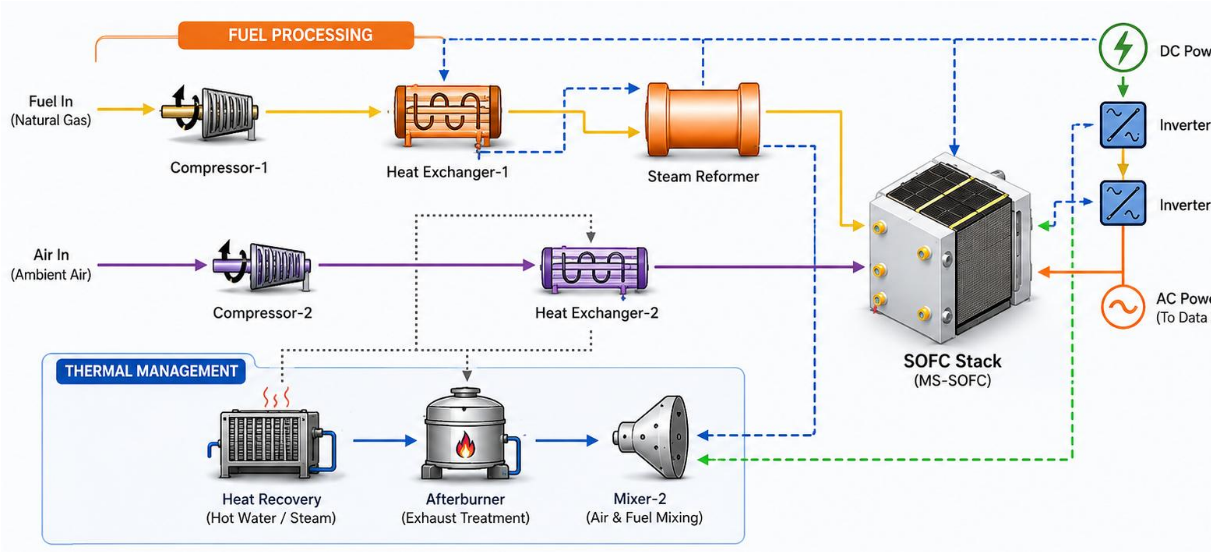

Mass balances
1. Fuel Channel
2. Air Channel
3. Chemical Reaction

Energy balances
1. Fuel Channel
2. Air Channel
3. PEN structure
4. Interconnect

Electrochemical
1. Nernst equation
2. Ohmic Overpotential
3. Concentration Polarization
4. Activation loss

Other components

Source

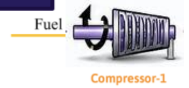

Ideal gas law
Peng-Robinson Equation of State (PR-EOS)

Reformer Afterburner

Equilibrium reactor
Energy balance
Mass balance

Heater Heat Exchanger

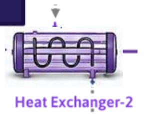

Energy balance
Mass balance

Simulink Modeling
MS-SOFC

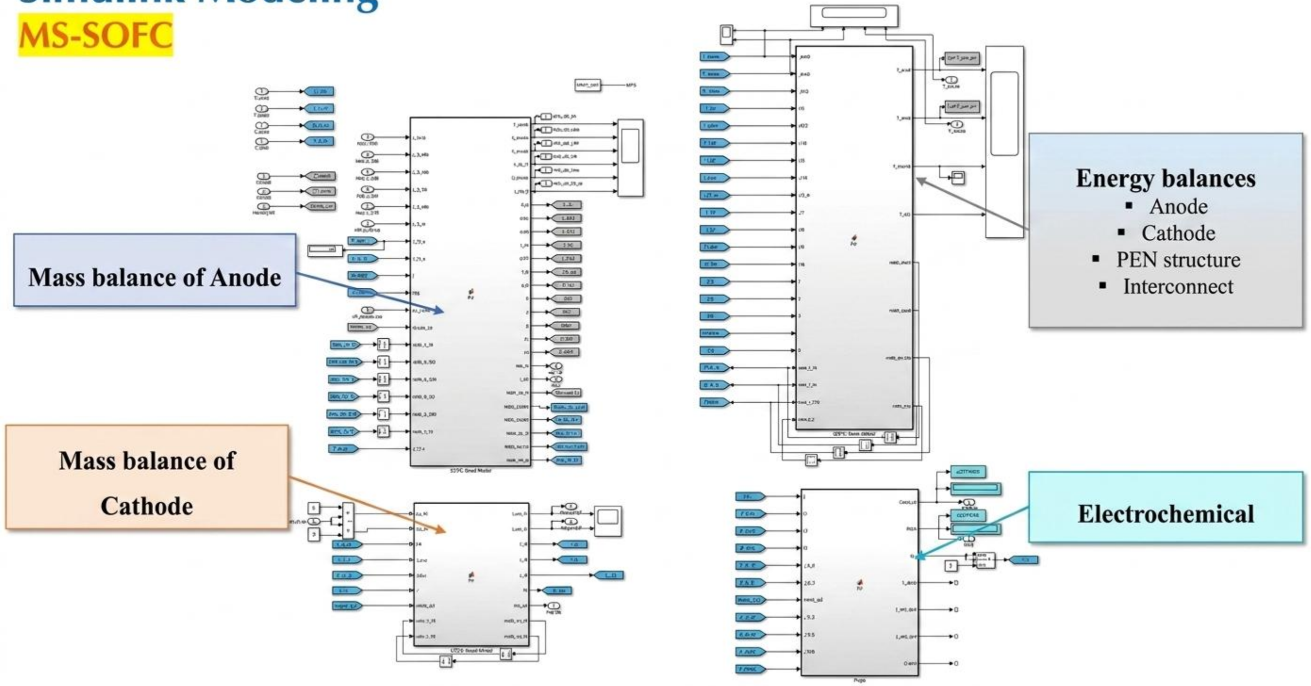

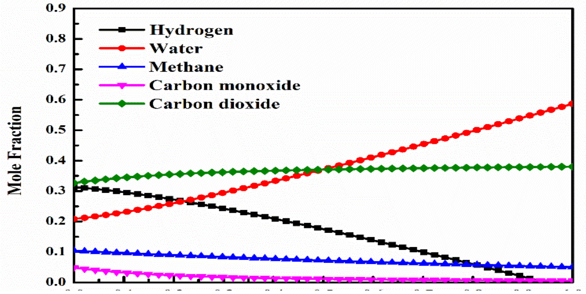

Energy Technology

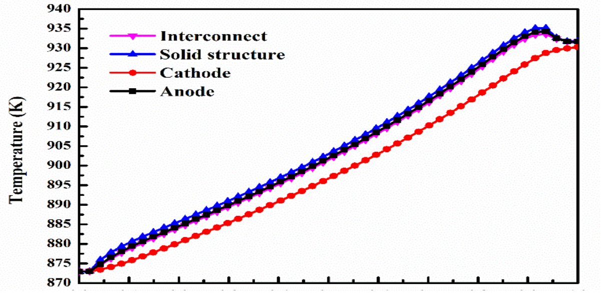

Energy Technology
Generation, Conversion, Storage, Distribution

RESEARCH ARTICLE OPEN ACCESS

Performance Analysis of Pure Hydrogen and Mixed Fuels in Medium-Temperature Metal-Supported Solid Oxide Fuel Cell

Jenn-Kun Kuo[1] | Ping-Hao Liu[1] | Sen-Wu Chiang[2] | Wen-Hsin Shen[2] | Wei-Cheng Wang[3]

[1]Department of Mechanical and Electro-Mechanical Engineering, National Sun Yat-sen University, Kaohsiung, Taiwan | [2]Hydrogen Energy Business Development, Delta Electronics, Incorporation, Tainan, Taiwan | [3]Department of Aeronautics and Astronautics, National Cheng Kung University, Tainan, Taiwan

HIL (Hardware in the Loop) Test Platform Fuel Cell Thermal System

HIL (Hardware-in-the-Loop) Test Platform Experimental Setup

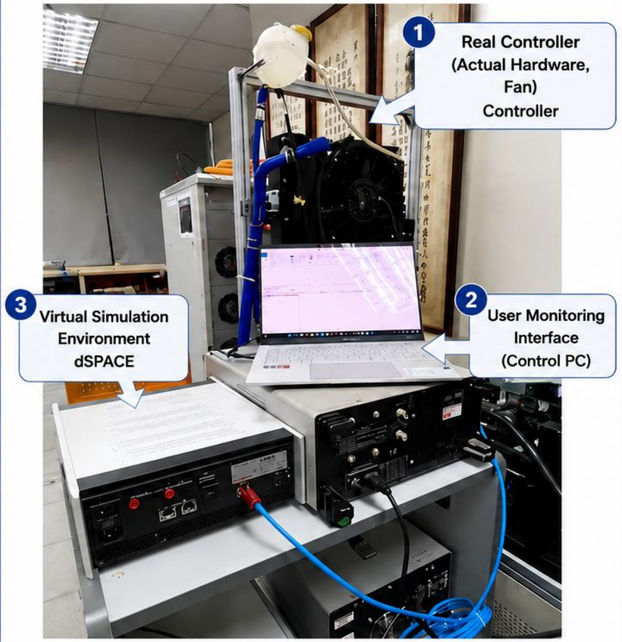

HIL (Hardware-in-the-Loop) Test Platform

Integrates real hardware, dSPACE real-time simulator, and control PC to validate control strategies and system behavior.

HIL (Hardware-in-the-Loop) Test Platform Experimental Setup

1 **MATLAB/Simulink** (Algorithm & Model Design Layer)

2 **ControlDesk** (Operation, Monitoring & Test Layer)

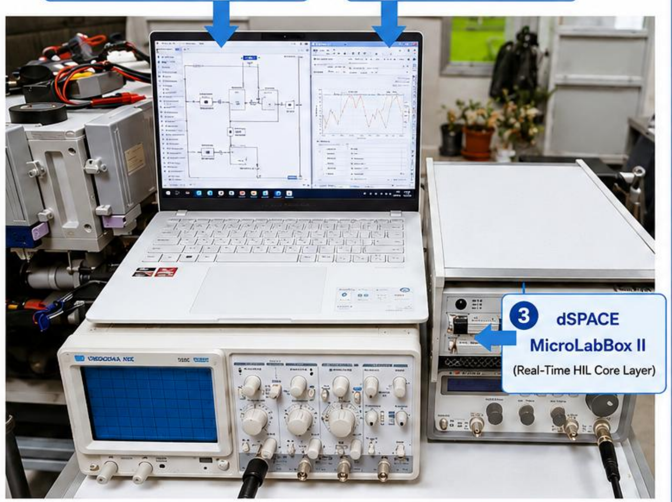

HIL (Hardware-in-the-Loop) Test Platform

Integrates MATLAB/Simulink, dSPACE MicroLabBox II, and ControlDesk to implement model operation, real-time control, data monitoring, and validation of control strategies and system behavior.

Hardware-in-the-Loop (HIL) Simulation — Signal Flow

Real ECU ↔ dSPACE Virtual Plant (Fuel Cell & Thermal System)

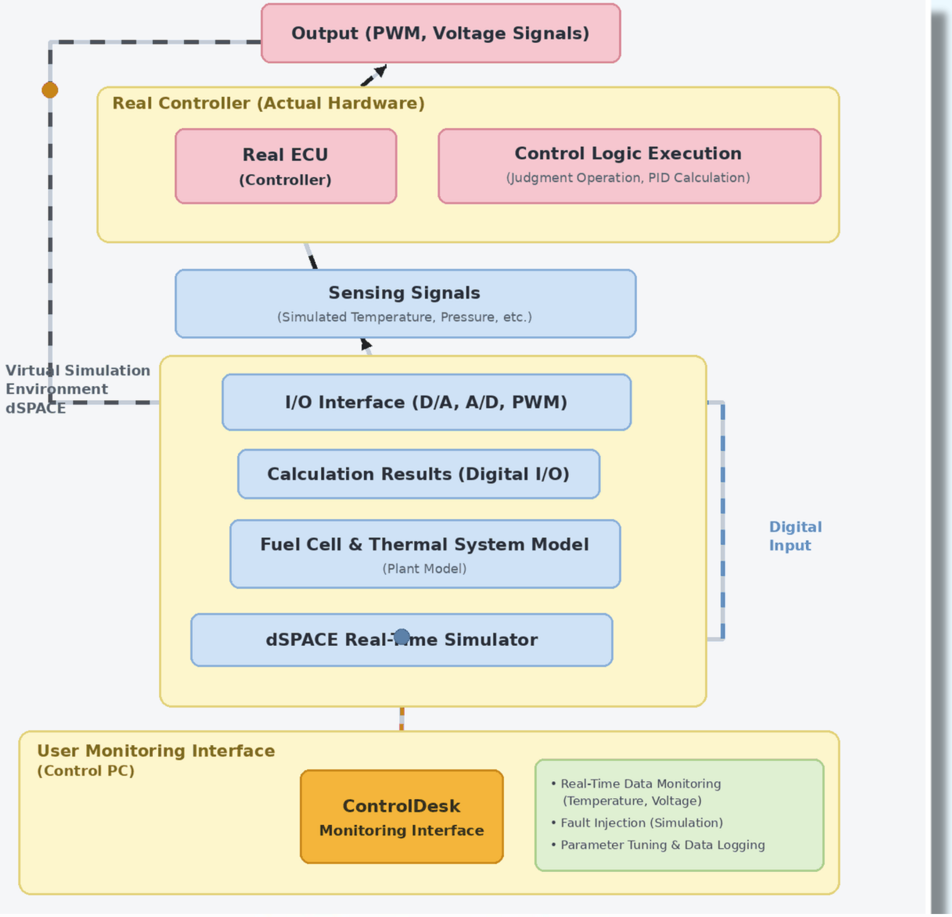

dSPACE MicroLabBox II Hardware / Simulator I/O Interface Configuration

- High-performance real-time simulator platform
- Rich I/O interface support
- Modular design, flexible extension
- Support multiple communication protocols

(Hardware in Loop, HIL) Hardware-in-the-Loop System Architecture

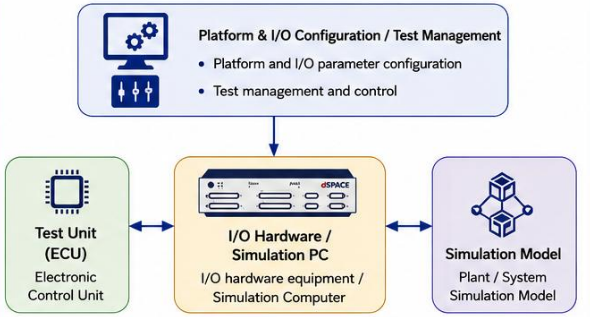

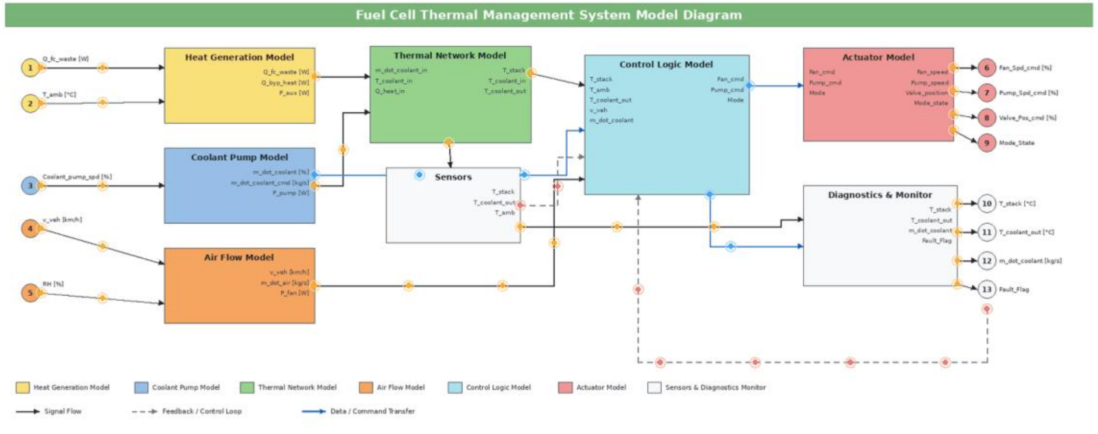

AI Data server's heat transfer

- **Computational Fluid Dynamics (CFD)**
- **Single-Phase Immersion Cooling (SPIC)**
- **Analysis of Heat Dissipation Performance**

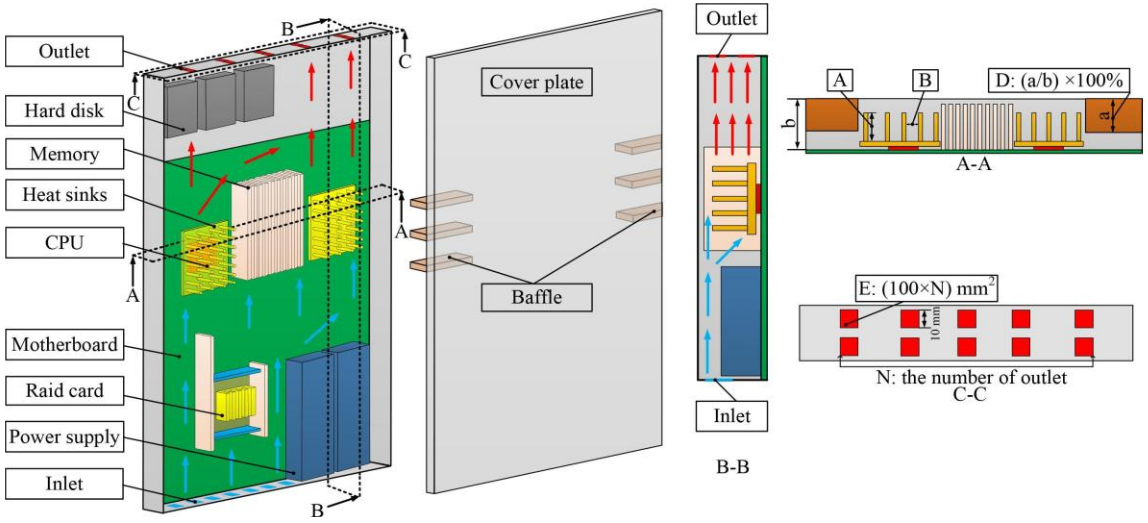

Internal component layout, airflow path, and baffle configuration

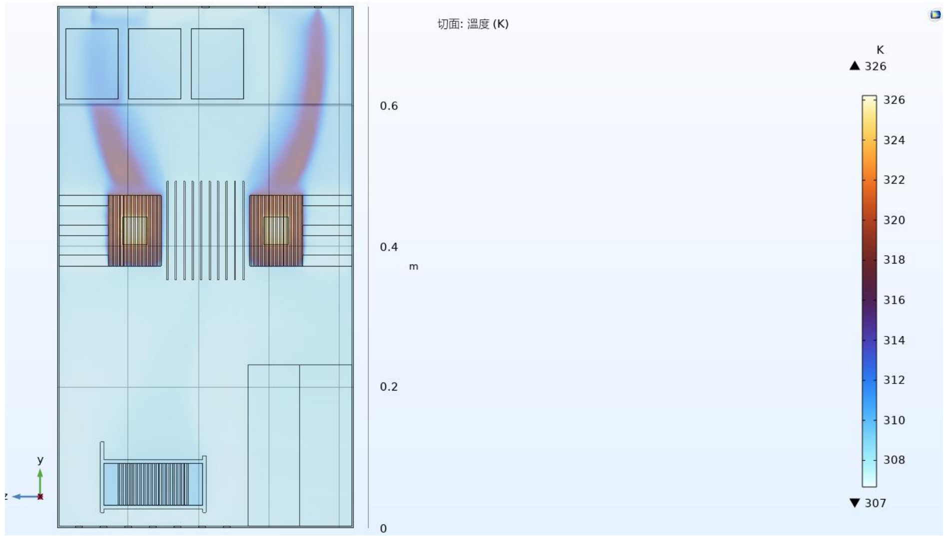

Simulated steady-state temperature distribution

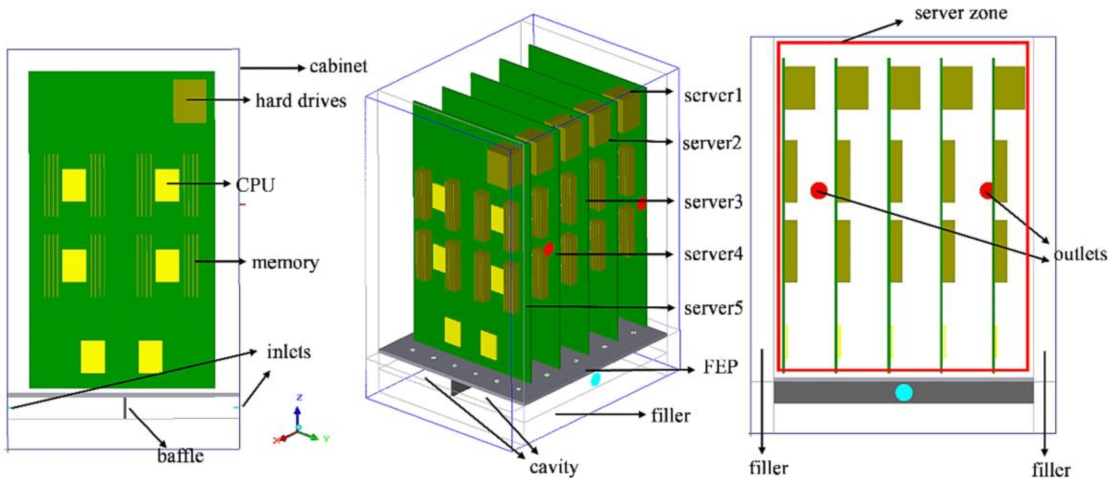

Server Cabinet Configuration Adopted from the Literature

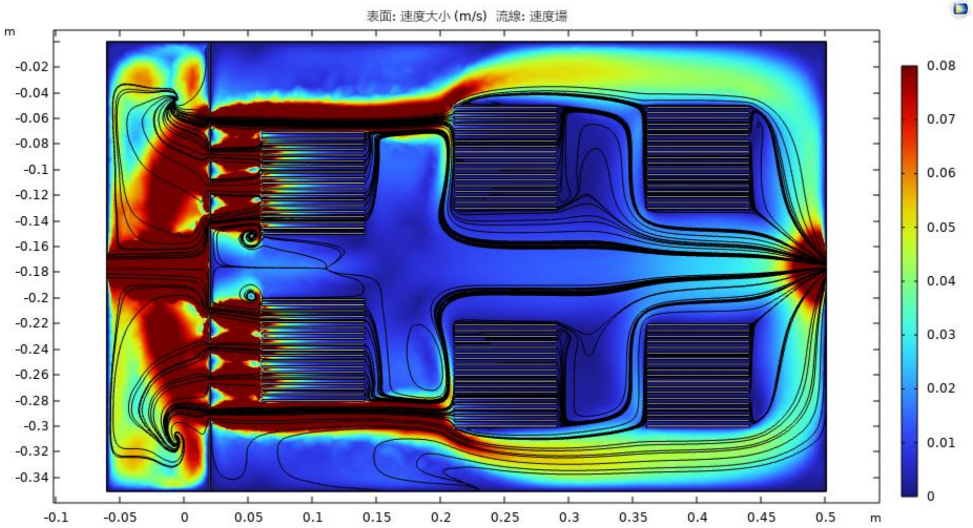

Coolant Velocity Distribution and Flow Streamlines

Semiconductor package structure（ASE Technology Holding Co. ）

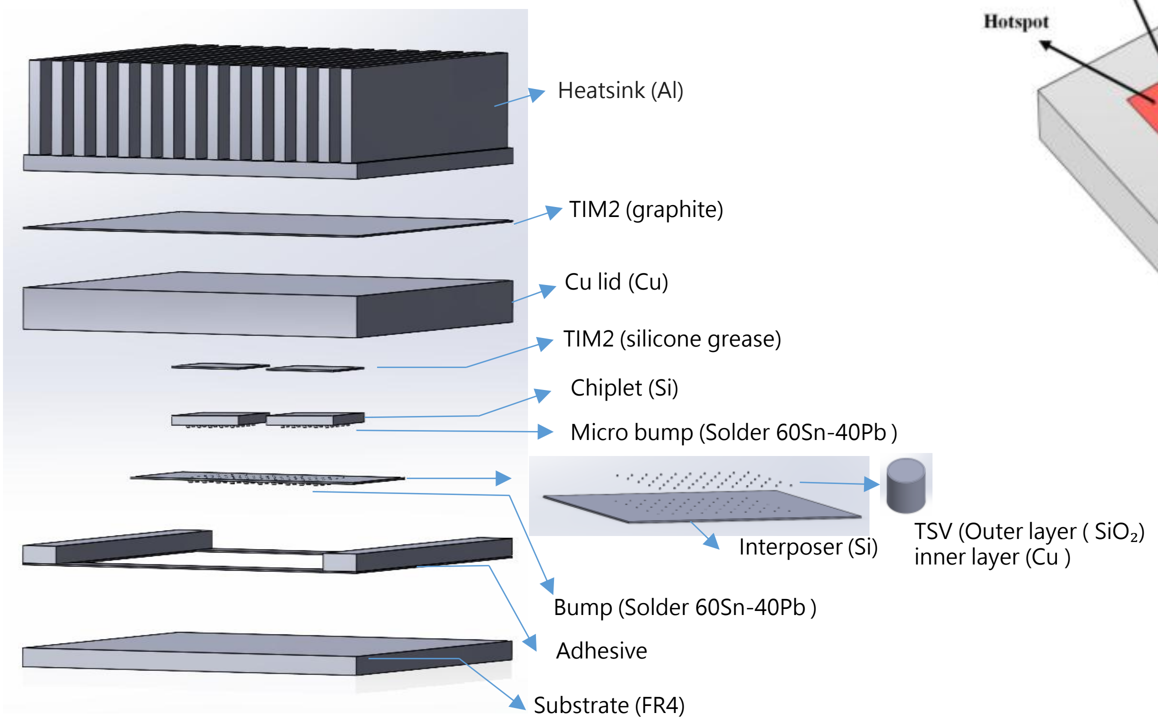

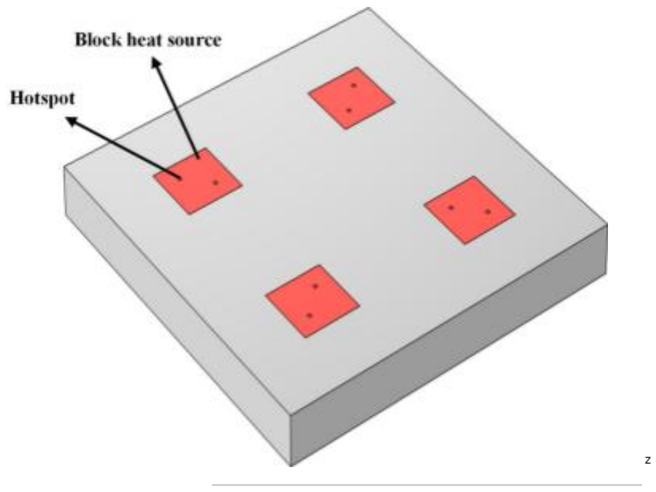

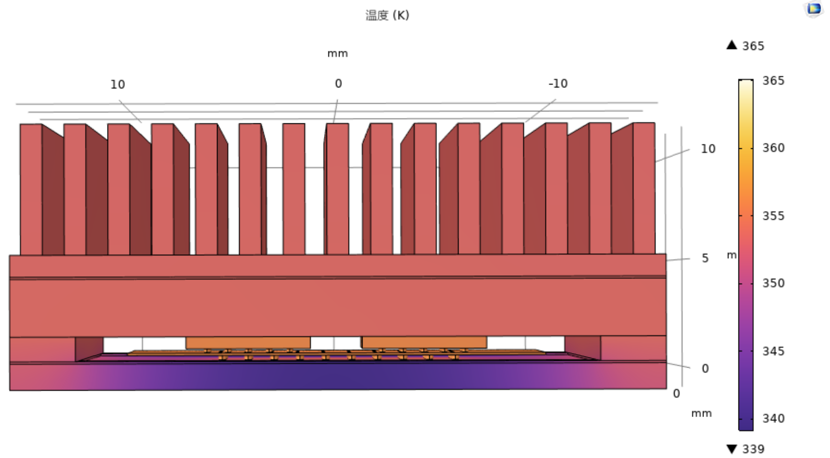

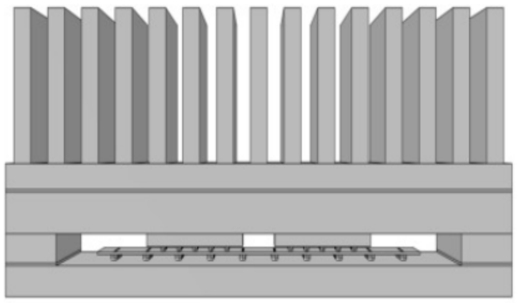

Simulation conditions :

Chiplet spacing	2.5 mm
Bump spacing	1.0 mm
Chiplet Volumetric heat source	2e7 W/m^3
Block heat source	2e5 W/m^2
Hotspot	4e7 W/m^2
Heatsink Surface convection heat transfer coefficient	h = 10 W/m^2K
Substrate Surface convection heat transfer coefficient	h = 2 W/m^2K
Initial/Ambient Temperature	293.15 K

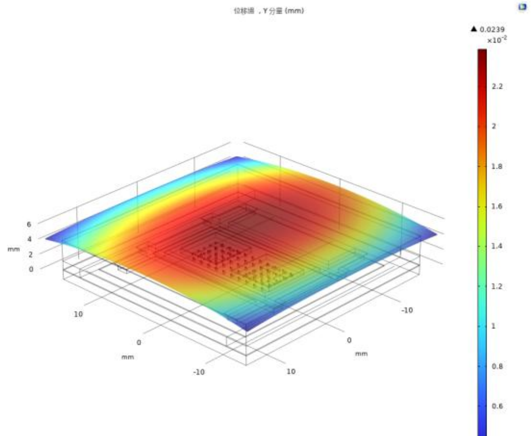

bending

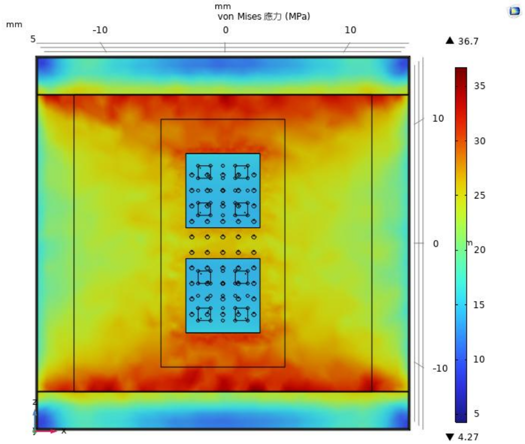

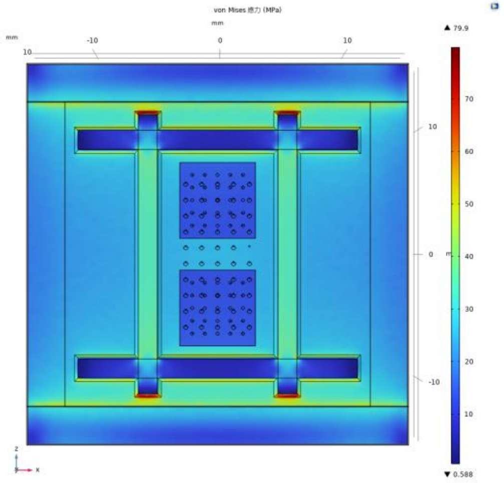

2025 H2 Energy and Fuel Cell Conference in Taiwan

Laboratory Team Members

Thank you for your attention!

Email: jenn.kun@gmail.com